



Colony formation in *Phaeocystis antarctica*: connecting molecular mechanisms with iron biogeochemistry

Sara J. Bender^{1,a}, Dawn M. Moran¹, Matthew R. McIlvin¹, Hong Zheng², John P. McCrow², Jonathan Badger^{2,b}, Giacomo R. DiTullio⁴, Andrew E. Allen^{2,3}, and Mak A. Saito¹

¹Marine Chemistry and Geochemistry Department, Woods Hole Oceanographic Institution, Woods Hole, Massachusetts 02543, USA

²Microbial and Environmental Genomics, J. Craig Venter Institute, La Jolla, California 92037, USA

³Integrative Oceanography Division, Scripps Institution of Oceanography, UC San Diego, La Jolla, California 92037, USA

⁴College of Charleston, Charleston South Carolina 29412, USA

^acurrent address: Gordon and Betty Moore Foundation, Palo Alto, California 94304, USA

^bcurrent address: Center for Cancer Research, Bethesda, Maryland 20892, USA

Correspondence: Mak A. Saito (msaito@whoi.edu)

Received: 2 January 2018 – Discussion started: 26 January 2018

Revised: 21 July 2018 – Accepted: 26 July 2018 – Published: 21 August 2018

Abstract. *Phaeocystis antarctica* is an important phytoplankton of the Ross Sea where it dominates the early season bloom after sea ice retreat and is a major contributor to carbon export. The factors that influence *Phaeocystis* colony formation and the resultant Ross Sea bloom initiation have been of great scientific interest, yet there is little known about the underlying mechanisms responsible for these phenomena. Here, we present laboratory and field studies on *Phaeocystis antarctica* grown under multiple iron conditions using a coupled proteomic and transcriptomic approach. *P. antarctica* had a lower iron limitation threshold than a Ross Sea diatom *Chaetoceros* sp., and at increased iron nutrition ($> 120 \text{ pM Fe}^{\prime}$) a shift from flagellate cells to a majority of colonial cells in *P. antarctica* was observed, implying a role for iron as a trigger for colony formation. Proteome analysis revealed an extensive and coordinated shift in proteome structure linked to iron availability and life cycle transitions with 327 and 436 proteins measured as significantly different between low and high iron in strains 1871 and 1374, respectively. The enzymes flavodoxin and plastocyanin that can functionally replace iron metalloenzymes were observed at low iron treatments consistent with cellular iron-sparing strategies, with plastocyanin having a larger dynamic range. The numerous isoforms of the putative iron-starvation-induced protein (ISIP) group (ISIP2A and ISIP3) had abundance patterns coinciding with that of either low or

high iron (and coincident flagellate or the colonial cell types in strain 1871), implying that there may be specific iron acquisition systems for each life cycle type. The proteome analysis also revealed numerous structural proteins associated with each cell type: within flagellate cells actin and tubulin from flagella and haptonema structures as well as a suite of calcium-binding proteins with EF domains were observed. In the colony-dominated samples a variety of structural proteins were observed that are also often found in multicellular organisms including spondins, lectins, fibrillins, and glycoproteins with von Willebrand domains. A large number of proteins of unknown function were identified that became abundant at either high or low iron availability. These results were compared to the first metaproteomic analysis of a Ross Sea *Phaeocystis* bloom to connect the mechanistic information to the in situ ecology and biogeochemistry. Proteins associated with both flagellate and colonial cells were observed in the bloom sample consistent with the need for both cell types within a growing bloom. Bacterial iron storage and B₁₂ biosynthesis proteins were also observed consistent with chemical synergies within the colony microbiome to cope with the biogeochemical conditions. Together these responses reveal a complex, highly coordinated effort by *P. antarctica* to regulate its phenotype at the molecular level in response to iron and provide a window into the biology, ecology, and biogeochemistry of this group.

1 Introduction

The genus *Phaeocystis* is a cosmopolitan marine phytoplankton group that plays a key role in global carbon and sulfur cycles (Hamm et al., 1999; Matrai et al., 1995; Rousseau et al., 2007; Schoemann et al., 2005; Smith et al., 1991; Solomon et al., 2003; Thingstad and Billen, 1994; Verity et al., 2007). Because of their large cell concentrations during bloom formation, *Phaeocystis* have a significant impact on the ocean biogeochemistry through carbon fixation (Arrigo et al., 1999; Hamm et al., 1999; Matrai et al., 1995; Rousseau et al., 2007; Schoemann et al., 2005; Smith et al., 1991; Solomon et al., 2003; Thingstad and Billen, 1994; Verity et al., 2007), the release of large concentrations of organic carbon upon grazing and viral lysis (Alderikamp et al., 2007; Hamm et al., 1999; Lagerheim, 1896; Verity et al., 2007), and export as aggregates out of the photic zone (DiTullio et al., 2000). Through the production of dimethylsulfide (DMS), they also directly connect ocean and atmospheric processes and carbon and sulfur cycling (Smith et al., 2003).

Some *Phaeocystis* species, including *Phaeocystis antarctica*, undergo multiple morphotypes and can occur as flagellated single cells or in gelatinous colonies consisting of thousands of non-motile cells (Fig. 1). Microscopic and chemical analyses have found that *Phaeocystis* colonies are filled with a mucilaginous matrix surrounded by a thin but strong hydrophobic skin (Hamm, 2000; Hamm et al., 1999). Once formed, cells typically associate with this outer layer of the colony (Smith et al., 2003). Colony formation involves the exudation of (muco)polysaccharides and carbohydrate-rich dissolved organic matter, as well as amino sugars and amino acids; it is estimated that approximately 50%–80% of *Phaeocystis* carbon is allocated to this extracellular matrix (Hamm et al., 1999; Matrai et al., 1995; Rousseau et al., 2007; Solomon et al., 2003; Thingstad and Billen, 1994). Thus, not only does the colony increase the size of *Phaeocystis* by several orders of magnitude, but the extracellular matrix material also constitutes the majority of measured algal (carbon) biomass (Rousseau et al., 1990). The colonial form of *Phaeocystis* has been suggested as a defense mechanism against grazers (Hamm et al., 1999), a means to sequester micronutrients such as iron and manganese (Lubbers et al., 1990; Schoemann et al., 2001), a means of protection from pathogens (Hamm, 2000; Jacobsen et al., 2007), and as a microbiome vitamin B₁₂ source (Bertrand et al., 2007). Colony formation of *Phaeocystis* species, including *P. antarctica* and *P. globosa*, has been linked to numerous physiological triggers including the synergistic effects of iron and irradiance (Feng et al., 2010), grazer-induced chemical cues (Long et al., 2007), phosphate concentrations (Riegman et al., 1992), and the presence of different nitrogen species (Riegman and van Boekel, 1996; Smith et al., 2003).

The Ross Sea is one of the most productive regions of the Southern Ocean (Arrigo et al., 1999, 1998; Feng et al., 2010; Garcia et al., 2009; Sedwick and DiTullio, 1997), and the lat-

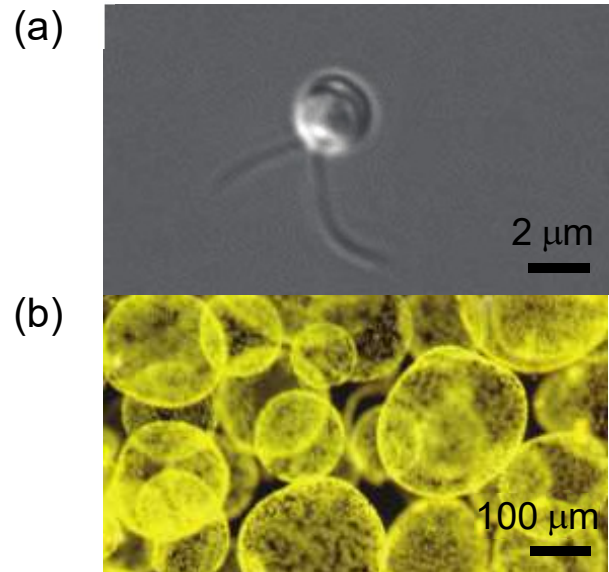


Figure 1. Micrographs of (a) a single *Phaeocystis* in cell culture and (b) *Phaeocystis* colonies in a Ross Sea bloom.

ter is an important contributor to the cycling of carbon in the oceans (Lovenduski et al., 2008; Sarmiento et al., 1998). In the early spring when the sea ice retreats and polynyas form, phytoplankton blooms and regional phytoplankton productivity are fed by the residual winter iron inventory and perhaps iron-rich sea ice melt (Noble et al., 2013; Sedwick and DiTullio, 1997); blooms have also been linked to changes in irradiance and mixed layer depth (Arrigo et al., 1999; Coale et al., 2003; Martin et al., 1990; Sedwick and DiTullio, 1997; Sedwick et al., 2000). In the Ross Sea polynya (RSP), *P. antarctica* colonial cells form almost monospecific blooms until the austral summer season begins, comprising >98% of cell abundance at the peak of the bloom (Smith et al., 2003). Although diatom abundance dominates in the summer, the RSP typically harbors the coexistence of flagellated single cells of *P. antarctica* along with diatoms (Garrison et al., 2003). During blooms *P. antarctica* can draw down more than twice as much carbon relative to phosphate as diatoms and contribute to rapid carbon export, leaving a lasting biogeochemical imprint on surrounding waters (Arrigo et al., 1999, 2000; DiTullio et al., 2000; Dunbar et al., 1998). Recent in vitro iron addition experiments provide evidence that iron nutrition influences *P. antarctica* growth in this region, with increasing *P. antarctica* biomass after iron addition (Bertrand et al., 2007; Feng et al., 2010). Moreover, laboratory experiments with *P. antarctica* have observed a high cellular iron requirement and variable use of strong organic iron complexes (Sedwick et al., 2007; Strzepek et al., 2011; Luxem et al., 2017).

The multiphasic life cycle of *P. antarctica* in the Ross Sea gives it a spectrum of nutrient drawdown phenotypes and trophic interactions dependent on the presence of flagellated versus colonial cells (Smith et al., 2003). Given its prominence during early spring sea ice retreat, it has been hypothesized that the triggers of colony formation for *Phaeocystis* cells are also the triggers of the spring phytoplankton bloom. Yet experimental and molecular analyses of potential environmental triggers and how they manifest in changes in cellular morphology have remained elusive. Little is known about the mechanisms responsible for colony formation in *P. antarctica* and how these mechanisms respond to an environmental stimulus such as iron, both of which appear to be integral to the ecology and biogeochemistry of *P. antarctica*.

2 Materials and methods

2.1 Culture experiments

Two strains of *Phaeocystis antarctica* (treated with Provasoli's antibiotics), CCMP 1871 and CCMP 1374 (Provasoli-Guillard National Center for Culture of Marine Phytoplankton), and a Ross Sea centric diatom isolate *Chaetoceros* sp. RS-19 (collected by Mark Dennett at 76.5° S, 177.1° W in December 1997 and isolated by Dawn Moran) were grown in F/2 media with a trace metal stock (minus FeCl₃) according to Sunda and Huntsman (Sunda and Huntsman, 1995, 2003) using a modified 10 μM EDTA concentration and an oligotrophic seawater base. Strains were chosen because they were culturable representatives from two distinct regions in the Southern Ocean.

Semicontinuous batch cultures were grown at 4 °C under 200 μmol photons m⁻² s⁻¹ of continuous light. Each strain was acclimated to the six iron growth condition concentrations for at least three transfers prior to proteome and growth rate experiments (>9 generations per transfer for >27 generations). The concentration of dissolved inorganic iron within each treatment was 2, 41, 120, 740, 1200, and 3900 pM Fe²⁺ as set by the metal buffer EDTA (where Fe²⁺ / Fe_{Total} = 0.039) (Sunda and Huntsman, 2003). During the experiment, cultures were maintained in 250 mL polycarbonate bottles, and subsamples were collected every 1–2 days in 5 mL 13 × 100 mm borosilicate tubes to measure relative fluorescence units (RFUs) and cell counts in the treatments. Mid-to-late exponential-phase cultures were harvested for transcriptome and proteome analysis and cell size was measured for both strains; cell pellets were stored at –80 °C (see the Supplement for additional methods). Cell counts were conducted using a Palmer–Maloney counting chamber and a Zeiss Axio Plan microscope on 400× magnification; cell numbers were used to determine the final growth rate of each strain and/or treatment. During mid-to-late exponential phase (time of harvest), cell size was determined for both strains (*n* = 20 cells were counted for each strain), as calculated using the Zeiss

4.8.2 software and a calibrated scale bar. The number of cells in colonies (versus as single cells) was determined for strain 1871 only. Briefly, counts (number of cells associated with colonies versus unassociated) were averaged from 10 fields of view at five distinct time points (50 fields of view total).

2.2 Protein extraction, digestion, and mass spectrometry analyses

Proteins from cell pellets (one pellet per treatment, two strains, and six iron treatments for a total of 12 proteomes) were extracted using the detergent B-PER (Thermo Scientific), quantified, purified by immobilization within an acrylamide tube gel, trypsin digested, alkylated and reduced, and analyzed by liquid chromatography–mass spectrometry (LC-MS) using a Michrom Advance HPLC with a reverse-phase C18 column (0.3 × 10 mm ID, 3 μm particle size, 200 Å pore size, SGE Protocol C18G; flow rate of 1 μL min⁻¹, nonlinear 210 min gradient from 5 % to 95 % buffer B, where A was 0.1 % formic acid in water and B was 0.1 % formic acid in acetonitrile; all solvents were Fisher Optima grade) coupled to a Thermo Scientific Q-Exactive Orbitrap mass spectrometer with a Michrom Advance CaptiveSpray source. The mass spectrometer was set to perform MS–MS on the top 15 ions using data-dependent settings (dynamic exclusion 30 s, excluding unassigned and singly charged ions), and ions were monitored over a range of 380–2000 *m/z* (see the Supplement for detailed protocol). Peptide-to-spectrum matching was conducted using the SEQUEST algorithm within Proteome Discoverer 1.4 (Thermo Scientific) using the translated transcriptomes for *P. antarctica* strain 1871 and strain 1374 (Fig. 2, see below). Normalized spectral counts were generated from Scaffold 4.0 (Proteome Software Inc.), with a protein false discovery rate (FDR) of 1.0 %, a minimum peptide score of 2, and a peptide probability threshold of 95 %. Spectral counts refer to the number of peptide-to-spectrum matches that are attributed to each predicted protein from the transcriptome analysis, and the Scaffold normalization scheme involves a small correction normalizing the total number of spectra counts across all samples to correct for run-to-run variability and improve comparisons between treatments. The R package “FactoMineR” (Lê et al., 2008) was used for the PCA; for heatmaps, the package “gplots” was used (Warnes et al., 2009). Proteomic samples taken from each laboratory condition were not pooled downstream as part of the analyses; replicates shown for each treatment are technical replicates.

2.3 RNA extraction, Illumina sequencing, and annotation

For *P. antarctica* cultures total RNA was isolated from cell pellets (one pellet per treatment, two strains, and three iron concentrations for a total of six transcriptomes) following the TRIzol Reagent (Life Technologies, manufacturer's

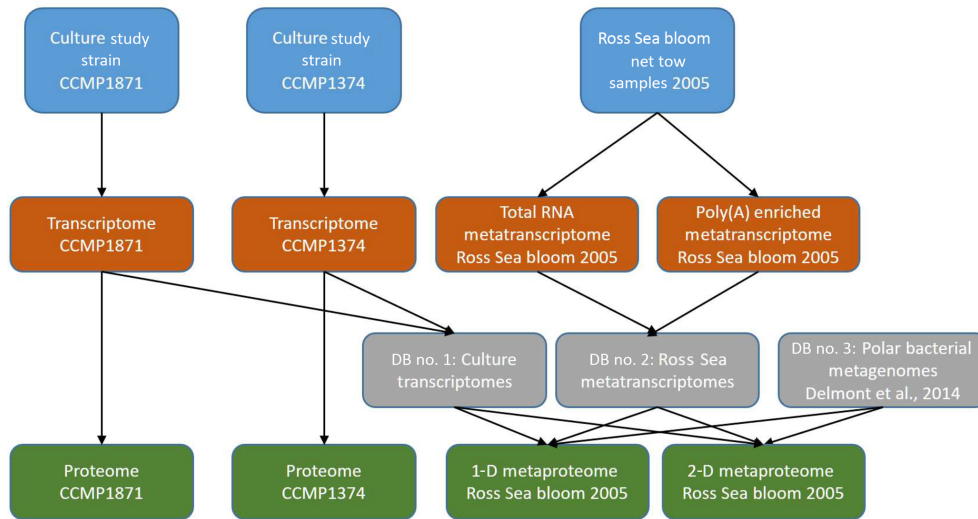


Figure 2. Experimental workflow used in this study. Culture and field samples (top), transcriptome analyses (second row), sequence database construction for proteomics (third row), and proteomic and metaproteomic analyses (bottom row).

protocol). RNeasy Mini Kit (Qiagen) was used for RNA cleanup, and DNase I (Qiagen) treatment was applied to remove genomic DNA. Libraries from poly(A) enrichment mRNA were constructed using a TruSeq RNA Sample Preparation Kit V2 (IlluminaTM), following the manufacturer's TruSeq RNA Sample Preparation Guide. Sequencing was performed using the Illumina HiSeq platform. Downstream, reads were trimmed for quality and filtered. CLC Assembly Cell (CLCbio) was used to assemble contigs, open reading frames (ORFs) were predicted from the assembled contigs using FragGeneScan (Rho et al., 2010), and additional rRNA sequences were removed. The remaining ORFs were annotated de novo via KEGG, KO, KOG, Pfam, and TigrFam assignments. Taxonomic classification was assigned to each ORF and the lineage probability index (LPI, as calculated in Podell and Gaasterland, 2007). ORFs classified as haptophytes were retained for downstream analyses. Analysis of sequence counts ("ASC") was used to assign normalized fold change and determine which ORFs were significantly differentially expressed in pairwise comparisons between treatments. The ASC approach offers a robust analysis of differential gene expression data for non-replicated samples (Wu et al., 2010).

For metatranscriptomes, RNA was extracted from frozen cell pellets using the TRIzol reagent manufacturer's protocol (Thermo Fisher Scientific) (see the Supplement for additional details on metatranscriptome processing).

2.4 Ross Sea *Phaeocystis* bloom: sample collection and protein extraction and analysis

The meta'omics samples were collected in the Ross Sea (170.76° E, 76.82° S) during the CORSACS expedition (Controls on Ross Sea Algal Community Structure) on

30 December 2005 (near pigment station 137; <http://www.bco-dmo.org/dataset-deployment/453377>, last access: 1 July 2018) (Saito et al., 2010; Sedwick et al., 2011). Surface water was concentrated via a plankton net tow (20 µm mesh), gently decanted of extra seawater, then split into multiple replicate cryovials and frozen in RNAlater at −80 °C for metatranscriptome and metaproteome analysis. The pore size of the net tow would have preferentially captured the colony form of *Phaeocystis*, although filtration with small pore size membrane filters was particularly challenging during this time period due to the abundance of *Phaeocystis* colonies and the clogging effect of their mucilage. Moreover, the physical process of deploying the net tow appears to have entrained some smaller cells including the *Phaeocystis* flagellate cells by adsorption to partially broken colonies and associated mucilage as observed in the metaproteome results. Two of these replicate bloom samples were frozen for proteome analysis. A third replicate sample from this field site was extracted for metatranscriptome analysis as described above.

Proteins were extracted, digested, and purified following the lab methods above and then identified first on a Thermo Q-Exactive Orbitrap mass spectrometer using a Michrom Advance CaptiveSpray source. Then samples were subsequently rerun on a two-dimensional chromatographic nanoflow system for increased metaproteomic depth on a Thermo Fusion Orbitrap mass spectrometer (see the Supplement for further details). Proteins were then identified within the mass spectra using three databases (Fig. 2): the translated transcriptome database for both *Phaeocystis* strains (Database 1), a Ross Sea metatranscriptome generated in parallel from this metaproteome sample (Database 2; this transcriptome is a combination of eukaryotic and prokaryotic communities derived from total RNA and poly(A) en-

riched RNA sequencing), and a compilation of five bacterial metagenomes from the Amundsen Sea polynya (Database 3) (Delmont et al., 2014) using SEQUEST within Proteome Discoverer 1.4 (Thermo Scientific) (Eng et al., 1994) and colated with normalized spectral counts in Scaffold 4.0 (Proteome Software Inc.) (see the Supplement for additional details).

3 Results and discussion

3.1 Physiological response to iron availability: growth limitation and colony formation

The two strains of *P. antarctica* (1374 and 1871 from here on) were acclimated to six iron concentrations to capture the metabolic response under different iron regimes (Fig. 3a and b). A biphasic response in *P. antarctica* strain 1871 was observed; cultures exhibited a clear single-cell versus colony response to low and high iron, respectively, that was observed by microscopy and readily apparent to the naked eye due to the millimeter size of the colonies. The three low iron treatment (2 pM, 41 pM, and 120 pM Fe³⁺) cultures contained only single, flagellated cells, whereas the three higher iron treatments (740 pM, 1200 pM, and 3900 pM Fe³⁺) had a majority of colonial cells based on detailed microscopy counts shown in Fig. 3c. This influence of iron on colony abundance was observed in an additional experiment, in which colonial cells were again absent at the lowest three iron concentrations and were present at the three higher concentrations (Fig. S10). The presence of both colony and flagellate cells is expected in actively growing populations since reproduction can involve returning to the flagellate life cycle stage (Rousseau et al., 1994). Single cells and colonies were not counted in experiments with strain 1374, as these experiments were conducted prior to those of 1871 and the iron-induced colony formation observations therein. However, strain 1374 was observed to become “clumpy” at high iron. This clumping observation may reflect the loss of a specific factor needed for the colony completion lost during long-term maintenance in culture. This interpretation is consistent with the overall similar structural protein expression patterns observed in both strains described below. Strzepek et al. also observed covarying of iron concentration and colony formation in some strains of *P. antarctica* (Strzepek et al., 2011).

The two strains of *P. antarctica* were able to maintain growth rates for all but the lowest of iron concentrations used here, similar to prior studies of *P. antarctica* strain AA1 that observed no effect of scarce iron on growth rates (Strzepek et al., 2011). Parallel experiments with polar diatoms such as *Chaetoceros* (Fig. 3d) observed growth limitation at moderate iron abundances using an identical media composition, indicating (1) that *P. antarctica* has an impressive capability for tolerating low iron compared to *Chaetoceros* and other

diatoms (e.g., a Ross Sea *Pseudo-nitzschia* sp. isolate, data not shown) and (2) demonstrating an absence of iron contamination in these experiments. Growth rates for 1871 were significantly different between the 2 pM Fe³⁺ treatment and all other treatments (Student's *t* test with Bonferroni correction, $p < 0.05$; Fig. 3a); there were no significant differences among growth rates for strain 1374 (Fig. 3b). Cell size (including both flagellate and colonial cells) decreased with lower iron concentration, a trend that was statistically significant (ANOVA with Tukey's HSD test, $p < 0.05$) for both strains when cell sizes from each high iron treatment (740 pM, 1200 pM, and 3900 pM Fe³⁺) were compared to cell sizes from each low iron treatment (2 pM, 41 pM, and 120 pM Fe³⁺) (Fig. 3e and f).

3.2 Molecular response to low and high iron concentrations

Global proteomics enabled by peptide-to-spectra matching to transcriptome analyses revealed a clear statistically significant molecular transition across the iron gradient for each strain (Fig. 4). The global proteome consisted of 536 proteins identified in strain 1871 and 1085 proteins identified in strain 1374 (Table 1; Supplement Data 1) after summing unique proteins across the six iron treatments. There were 55 proteins identified in strain 1871 and 64 proteins in strain 1374 (Fig. 4) that drove the statistical separation of proteomes across iron treatments using principal component analysis (PCA; axis 1 PCA correlation coefficient ≥ 0.9 or ≤ -0.9). Axis 1 accounted for 49 % of the variance for 1871 and 36 % of the variance for 1374. Moreover, using a Fisher test (p value ≤ 0.05), 327 (strain 1871) and 436 (strain 1374) of those proteins detected were identified as significantly different in relative protein abundance between representative “low” (41 pM Fe³⁺) and “high” (3900 pM Fe³⁺) iron treatments. This significant change in the proteome composition paralleled observations of a shift from flagellate to colonial cells. Iron-starvation responses and iron metabolism were detected within the high and low iron PCA protein subsets, including iron-starvation-induced proteins (ISIPs), flavodoxin, and plastocyanin, demonstrating a multifaceted cellular response to iron scarcity (Fig. 5). Surprisingly, there was also a highly pronounced signal in the proteome that appeared to reflect the structural changes occurring in *P. antarctica*. These structural proteins included multiple proteins with protein family (PFam) domains suggestive of extracellular function, adhesion, and/or ligand binding, including putative glycoprotein domains (for example, spondin) that were present in the high iron PCA subset in both strains (Fig. 5); the appearance of these proteins also corresponded to the occurrence of colonies in strain 1871 (Fig. 1). Similarly, a distinct suite of proteins was more abundant in the low iron PCA subset (Fig. 5), including proteins relating to cell signaling (for example, calmodulin–EF hand, PHD zinc ring finger). A number of proteins with unknown function were also detected in

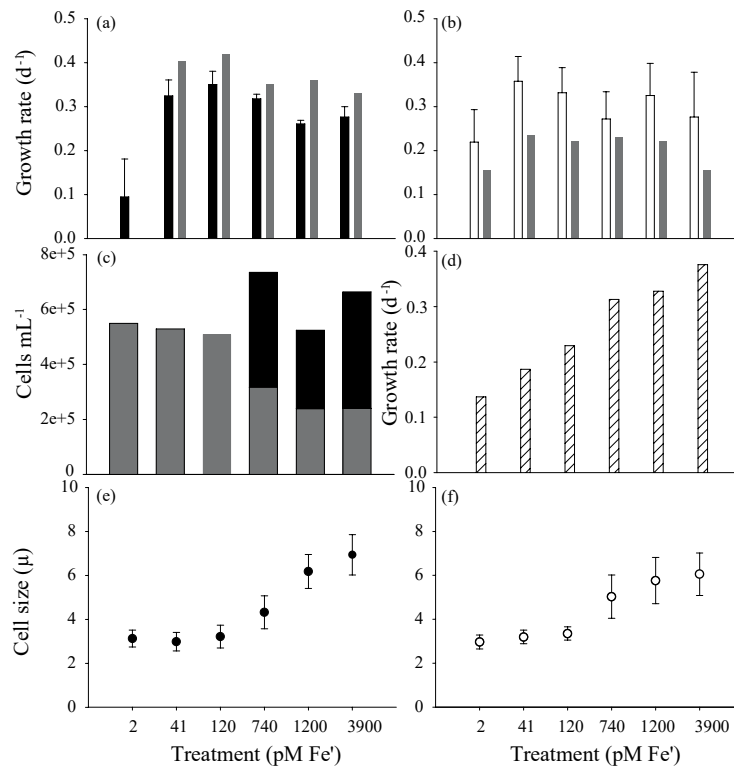


Figure 3. The effect of iron concentration on colony formation and cell physiology in two strains of *P. antarctica* – 1871 and 1374. Growth rates collected from acclimated culture stocks prior to the start of the experiments (**a**, strain 1871; **b**, strain 1374) calculated using relative fluorescence units from three transfers of acclimated cultures (error bars indicate SD, $n = 3$). Accompanying gray bars represent growth rates calculated based on cell counts made during the course of the proteome harvest experiments ($n = 1$). (**c**) The number of *P. antarctica* 1871 free-living cells (gray bars) compared to cells associated with colonies (black bars) showed a shift to a majority of colonial cells when $\text{Fe}^{3+} \geq 740$ pM. (**d**) The growth rate of Ross Sea diatom isolate *Chaetoceros* sp. strain RS-19 in the same media compositions ($n = 1$) demonstrated a higher sensitivity to iron scarcity and a lack of iron contamination in the media. Cell size for strain 1871 (**e**; black circles) and strain 1374 (**f**; white circles); error bars represent SD of $n = 20$ cell measurements per treatment.

the PCA subsets: 71 % unknown for strain 1871 and 42 % unknown for strain 1374 of a total of 311 proteins annotated as hypothetical proteins (Supplement Dataset 1). Outside of the PCAs, additional iron and adhesion-related proteins were identified that demonstrated a similar expression profile to the PCA subset (Supplement Fig. S1).

Identification and characterization of proteins and transcripts induced by iron scarcity are valuable in improving an understanding of the adaptive biochemical function of these complex phytoplankton as well as for their potential utility for development as environmental stress biomarkers (Roche et al., 1996; Saito et al., 2014). The enzymes flavodoxin and plastocyanin, which require no metal and copper, respectively, and that functionally replace iron metalloenzymes counterparts ferredoxin and cytochrome c6, had isoforms that increased in concentration in the lower iron treatments consistent with cellular iron-sparing strategies (Figs. 6, S2) (Peers and Price, 2006; Whitney et al., 2011; Zurbriggen et al., 2008). In strain 1374, however, there was an increase in both of these iron-sparing systems at the highest iron con-

centration (Fig. 6d and f, Supplement Table S1). While during both experiments cells were growing exponentially at the time of harvest, those of strain 1374 were as much as 7.6-fold denser in cell number than those of strain 1874 (based on cell counts from treatments specifically used for transcriptome analyses), and as a result the denser 1374 strain might have also experienced iron stress even at this highest iron concentration as the high biomass depleted iron within the medium. Of these two iron-sparing enzymes, plastocyanin appeared to show a clearer increase in abundance at lower environmental iron concentrations (Fig. 6c and f). In contrast, some flavodoxin isoforms could be interpreted as being constitutive; two of the three isoforms were still present in reasonable spectral counts at higher iron concentrations (Fig. 6a and d). Prior measurements during a Ross Sea colonial *P. antarctica* spring bloom in 1998 were consistent with this interpretation, with ferredoxin concentrations below detection and flavodoxin present (Maucher and DiTullio, 2003). A constitutive flavodoxin could help explain *P. antarctica*'s ability to tolerate all but the lowest iron treatment observed in the

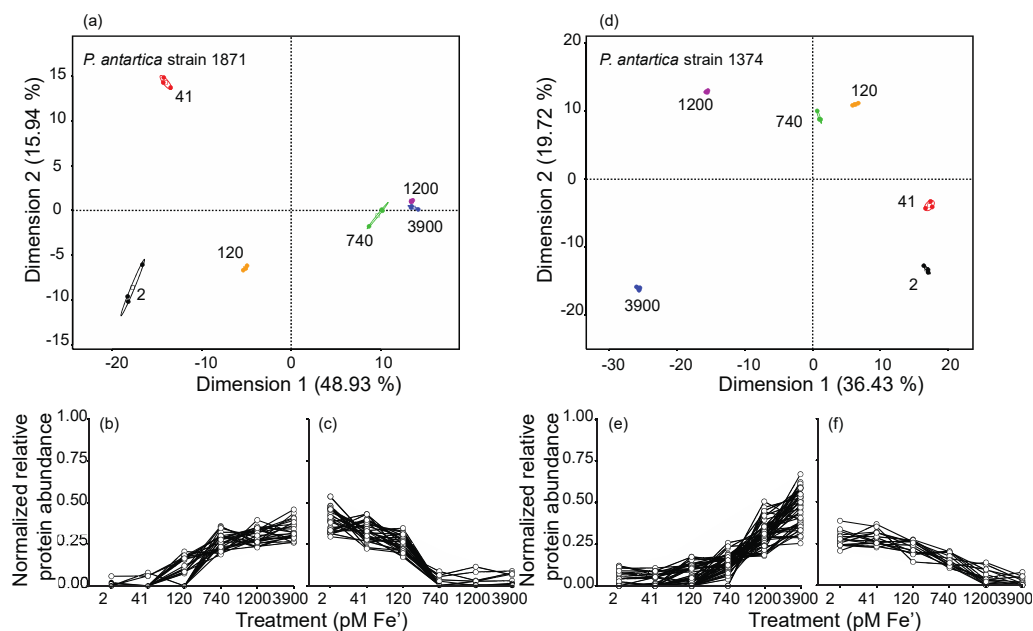


Figure 4. Principal component analysis (PCA) of the measured proteomes for each iron condition for strain 1871 and strain 1374 and corresponding line graphs highlighting the proteins driving the PCA separation (PCAs: ≥ 0.9 or ≤ -0.9). (a, d) Iron treatments (pM Fe[']) are highlighted by color (2, black; 41, red; 120, orange; 740, green; 1200, purple; 3900, blue) and large ellipses indicate confidence ellipses calculated using the R package FactoMineR. Each small solid circle represents a technical replicate per iron treatment ($n = 3$); colored open squares represent the mean of the iron treatment (empirical variance divided by the number of observations). Proteins with eigenvalues ≥ 0.9 or ≤ -0.9 are plotted in graphs b and c for strain 1871 and (e) and (f) for strain 1374 to highlight the subset of proteins driving the variance in Dimension 1. Individual protein spectral counts normalized to total spectral counts for all treatments for a given protein, written as “normalized relative protein abundance”, are plotted on the y axis. The six iron treatments (pM Fe[']) are plotted from low to high (left to right) on the x axis.

physiological experiments (Fig. 3a and b) and implies that the careful selection of isoforms, or better, the inclusion of all isoforms of a protein biomarker of interest may be valuable in interpreting complex field results.

There were also numerous isoforms of the iron-starvation-induced protein (ISIP) group identified within the proteome of each *P. antarctica* strain: specifically, nine ISIP2As and three ISIP3s in strain 1871 and three ISIP2As and four ISIP3s in strain 1374 (Fig. S1; Table S1). These ISIPs were identified based on their transcriptome response to iron stress in diatoms and most recently have been implicated in a diatom cell surface iron-concentrating mechanism (Allen et al., 2008; Morrissey et al., 2015). Interestingly in this *P. antarctica* experiment, these ISIPs exhibited both “high” and “low” iron responses, but specific isoforms were more abundant only under one of those respective conditions (Fig. 6). Given the metamorphosis of *P. antarctica* between flagellate and colonial cell types observed by microscopy and the proteome across the gradient in iron concentrations, we hypothesize that this diversity of iron stress responses in the ISIPs may reflect the complexity associated with *P. antarctica*'s life cycle. As the abundant winter iron and sloughed basal sea ice reserves are depleted, newly formed colonial cells will in-

evitably find themselves in the iron-depleted environments that have been characterized in the Ross Sea almost immediately upon bloom formation due to iron's small dissolved inventory (Bertrand et al., 2011, 2015; Sedwick et al., 2011). As a result, *P. antarctica* may have distinct iron stress protein isoforms associated specifically with the colonial cell type (such as the high iron and colonial ISIPs; Figs. 5 and 6) in order to acquire scarce iron during blooms, in addition to a distinct suite of iron stress proteins produced within the flagellate cells (low iron and flagellate ISIPs; Figs. 5 and 6). Given the rapid depletion of iron during Ross Sea blooms, it is also conceivable that these iron-acquisition proteins are constitutively expressed within the colony morphotype rather than being connected to an iron-sensing and regulatory response system. Future short-term iron perturbation studies that would complement the steady-state experiments presented here could further investigate this hypothesis. The multiplicity of ISIPs produced within each strain is also consistent with the observation that both *P. antarctica* strains maintained high growth rates, even at the lower 41 and 120 pM Fe['] concentrations, compared to the diatom *Chaetoceros* sp. whose growth rate is less than 50 % of maximal growth in similar media (Fig. 3).

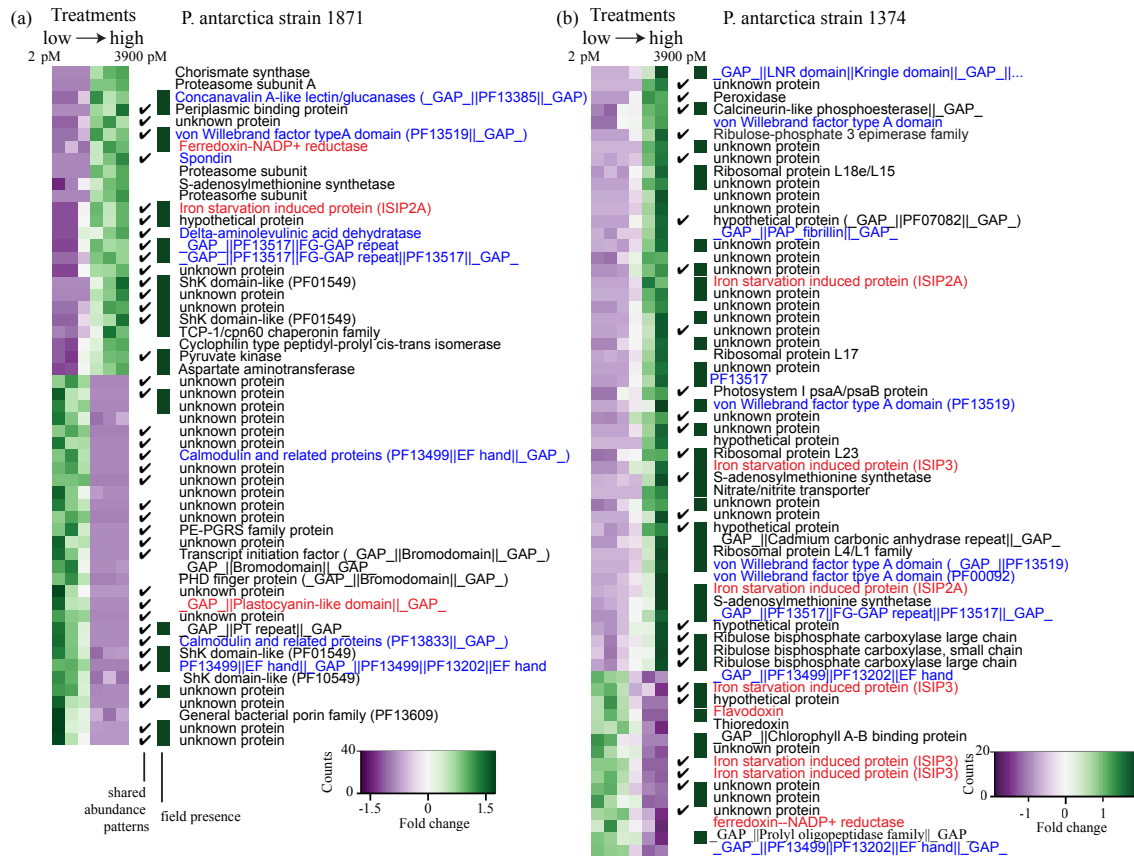


Figure 5. Heatmaps highlighting the relative protein abundance for the six treatments for *P. antarctica* strain 1871 (a) and strain 1374 (b). The darker green color indicates a greater relative abundance compared to the purple treatments. The “shared abundance patterns” column features a checkmark when a shared response to changes in iron availability between the relative protein abundance and the transcript abundance was observed (for example, both transcripts and proteins have a higher abundance under high iron compared to low iron growth or both transcripts and proteins have a higher abundance under low iron compared to high iron growth). The “field presence” column indicates whether or not that protein was detected in the field metaproteome (annotated using Database 1). Protein annotations are based on KEGG, KOG, and Pfam descriptions. Annotations in red are associated with iron metabolism and those in blue with cell adhesion and/or structure.

3.3 Correspondence between RNA and protein biomolecules

Many of the RNA transcripts of iron-related genes trended with their corresponding proteins: 60 % of the iron-related gene transcripts reflected the proteomic response in strain 1871, whereas there was a 30 % correspondence between iron-related transcripts and proteins in strain 1374 (Fig. S1). In total, 47 % of expressed proteins in strain 1871 and 26 % of proteins in strain 1374 shared expression patterns with associated transcripts (Fig. 7), consistent with recent studies of proteome–transcriptome comparisons that showed limited coordination between inventories of each type of biomolecule (Alexander et al., 2012). As mentioned above, while both experiments were in exponential growth at the time of harvest, strain 1374 was 7.6-fold denser in cell number than those of strain 1874 at that time. Hence, this decrease in transcript–proteome coherence in strain 1374 may be related to harvesting in the late-log growth phase and re-

flects the challenge of trying to conduct comparisons of these biomolecules that function on different cellular timescales.

Examination of the transcriptome revealed a significant increase in transcripts for tonB-like transporters, which can be associated with cross-membrane nutrient transport (e.g., for iron siderophore complexes or vitamin B₁₂; Bertrand et al., 2007, 2013; Morris et al., 2010) under high iron for strain 1871 and significantly greater transcript abundances for a putative flavodoxin for strain 1374 under low iron consistent with its substitution for ferredoxin due to iron scarcity (Roche et al., 1996).

3.4 Observation of an iron-induced switch from single cells to colonies

The strong connection of iron availability to putative structural components of *P. antarctica* observed here served as an ideal opportunity to examine the genes and proteins involved in morphological and life cycle transitions and colony con-

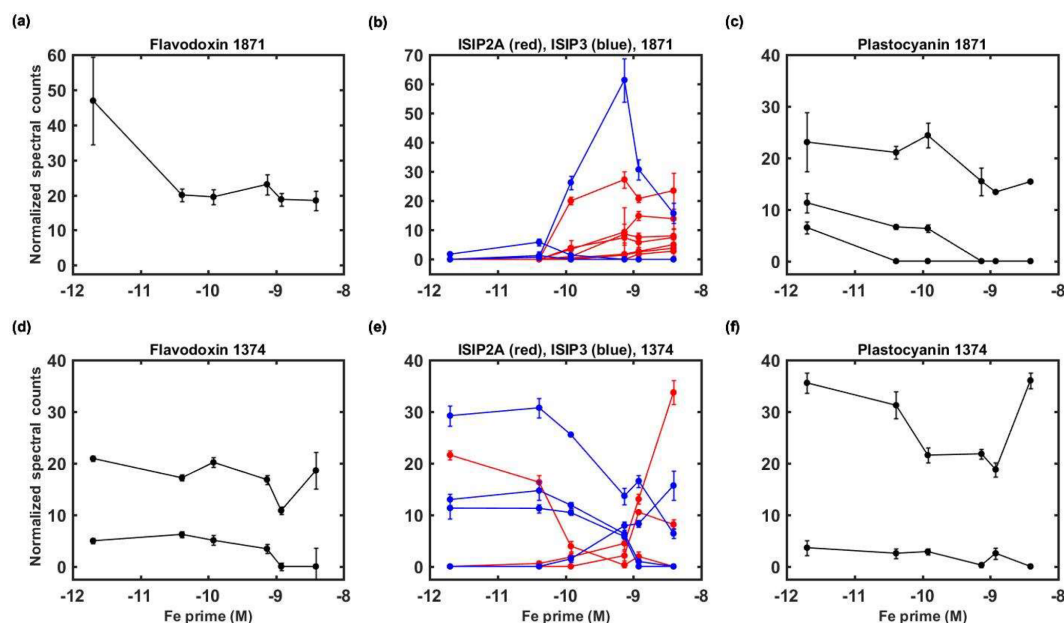


Figure 6. Examination of iron stress response proteins in *P. antarctica* strain 1871 (a, b, c) and 1374 (d, e, f). Relative protein abundance is shown as normalized spectral counts; spectral counts have been normalized across experiment treatments for each strain, but not to the maximum of each protein as used in prior figures to allow for comparison of abundance for similar isoforms. Error bars indicate the standard deviation of technical triplicate analyses.

struction in this phytoplankter that can otherwise be experimentally difficult to trigger in isolation. *Phaeocystis* colonies have captured the interest of scientists for more than a century (Hamm et al., 1999), yet next to nothing is known about the molecular basis of their construction. Colonies have been considered a collection of loosely connected cells embedded within a gel matrix and hence described as “balls of jelly” or “bags of water” (Hamm et al., 1999; Lagerheim, 1896; Verity et al., 2007). Results here suggest significant transformations in the cellular proteome that corresponded to solitary and colonial morphological stages, for example, involving structural proteins and proteins known to be post-translationally modified such as glycoproteins or those containing glycoprotein-binding motifs. To our knowledge, such an extensive proteome remodeling has yet to be observed for another colonial organism or with the influence of any other environmental stimuli in the genus *Phaeocystis*. As a result the details of this response, while fascinating, are challenging to interpret due to their novelty.

A putative spondin protein exhibited one of the largest responses between low and high iron in both strains with a greater than 20-fold increase in relative protein abundance and normalized 11-fold change in transcript abundance in strain 1871 and a greater than 9-fold increase in relative protein abundance and 3-fold change in transcript abundance in strain 1374 (Fig. 5a and Supplement Data 1). Spondin proteins are known to be glycosylated and to be a component of the extracellular matrix (ECM) environment, which may enable multicellularity in metazoans through cell adhesion,

and have been found to help coordinate nerve cell development through adhesion and repulsion (Michel et al., 2010; Tzarfati-Majar et al., 2011). Despite this large variation in protein abundance, the function of spondins in eukaryotic phytoplankton, including *Phaeocystis*, remains largely unknown. Given their responsiveness to iron availability and the associated enrichment in colony rich cultures, these proteins could potentially contribute to ECM-related adhesion of cells, to each other or the colony skin, or even perhaps to the mucilage interior.

Additional glycoproteins that exhibited a strong iron response in both strains include those containing von Willebrand factor domains (for example, protein families PF13519, PF00092) and fibrillin and lectin (Figs. 5 and S1). In biomineralizing organisms, such as corals, glycoproteins with von Willebrand domains are hypothesized to play a role in the formation of the extracellular organic matrix through adhesion (Drake et al., 2013; Hayward et al., 2011) by laying the scaffolding for calcification. Orthologs of the von Willebrand proteins that contain these domains have also been characterized in humans and have protein-binding capabilities, which are important for coagulation (Ewenstein, 1997). These dynamic von Willebrand proteins appear to contribute to the cell aggregation and colony formation of *P. antarctica* colonies.

The suite of structural and modified proteins described above demonstrates a means through which *P. antarctica*'s colonial morphotype could be constructed, and this dataset provides rare molecular evidence for the proteome recon-

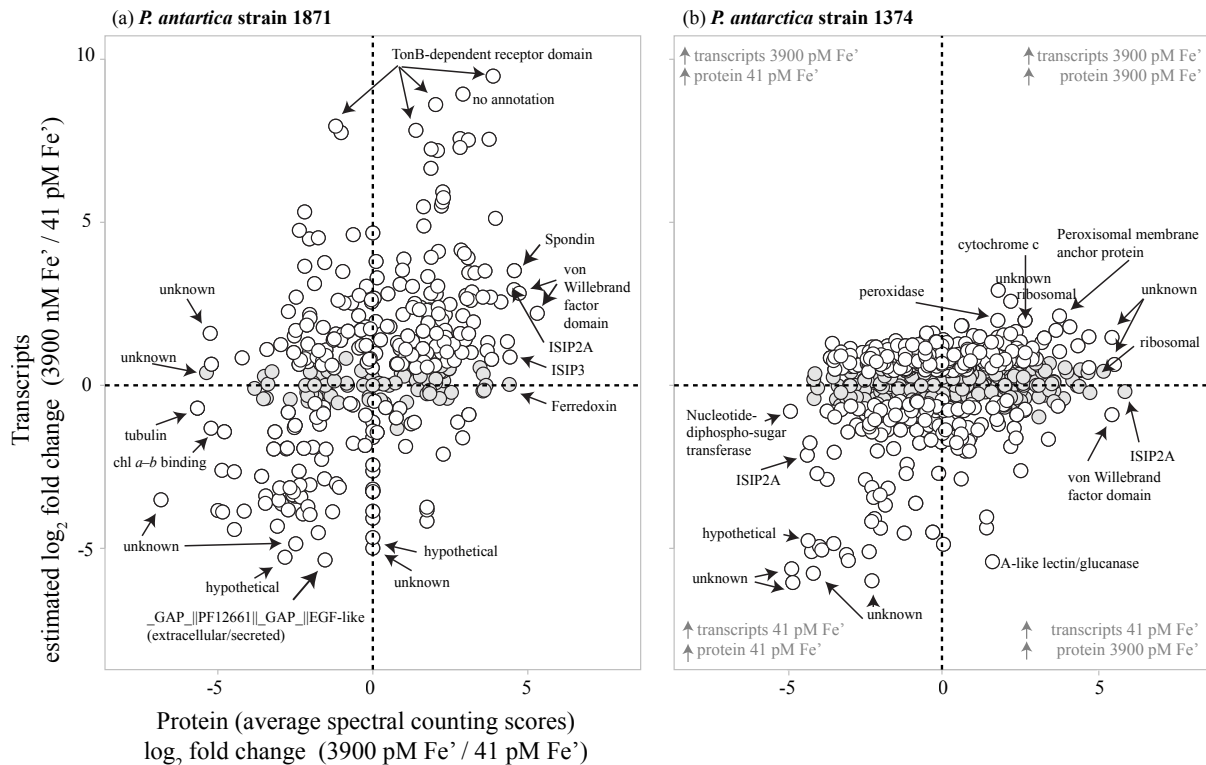


Figure 7. Scatterplots of relative transcript abundance (y axis) and relative protein abundance (x axis) for *P. antarctica* strain 1871 (a) and strain 1374 (b) for a high iron treatment (3900 pM Fe') relative to a low iron treatment (41 pM Fe'). Gray circles represent instances in which transcript abundance was not significantly different between conditions ($P \geq 0.99$). Quadrants in which relative protein and transcript abundances agree (upper right, lower left) and disagree (upper left, lower right) are noted, as are select genes exhibiting the greatest relative protein abundance and/or transcript abundance under a given treatment.

struction needed to switch between single organisms to a multicellular colony. The evolution of multicellularity in eukaryotes is an area of significant interest that has mostly focused on model organisms with colonial forms such as choanoflagellates and *Volvox* (Abedin and King, 2010). Genomic studies of the former identified the presence of protein families involved in cell interactions within metazoans, including C-type lectins, cadherins, and fibrinogen (King et al., 2003). In other lineages of microalgae that form colonial structures, such as *Volvox carteri*, there is supporting evidence for glycoproteins cross-linking within the extracellular matrix of colonies (Hallmann, 2003), as well as serving other important functional roles in cell–cell attachment during colony formation (for example, colony formation in the cyanobacteria *Microcystis aeruginosa*) and as an integral component of cell walls (for example, the diatoms *Navicula pelliculosa* and *Craspedostauros australis*) (Chiovitti et al., 2003; Kröger et al., 1994; Zilliges et al., 2008). In this study, environmental isolates of *P. antarctica* displayed consistent trends in similar protein families (for example, lectins, fibrillins, and glycoproteins), and they were produced at higher levels under elevated iron conditions when strain 1871 was primarily in colonial form. Given *P. antarctica*'s environ-

mental importance and ability to control the transition between flagellates and colony cell types through iron availability, *P. antarctica* may serve as a useful model for studying multicellularity in nature and in the context of environmental change.

In contrast to these putative colonial structural proteins, there were canonical cytoskeletal proteins such as actin and tubulin observed in *P. antarctica* cultures grown under low iron conditions (Fig. S1). These proteins were likely associated with the flagella and the haptonema, a shorter organelle containing nine microtubules that is characteristic of haptophytes (Zingone et al., 1999), found in the solitary *Phaeocystis* cell, and similar to other eukaryotic flagellar systems such as *Chlamydomonas* (Watanabe et al., 2004). Additionally, a suite of proteins with calcium-binding domains (EF-hand protein families) was identified in greater relative abundance under low iron growth conditions in both strains (Figs. 5, S1 and Supplement Data 1). In diatoms, calcium-signaling mechanisms have been directly linked with how cells respond to bioavailable iron, as well as stress responses (Allen et al., 2008; Vardi, 2008). Calcium (and magnesium) ions also play an integral role in the ability for extracellular mucus to gel (van Boekel, 1992). The greater abundance of putative

Table 1. Comparison of the total number of proteins and spectra measured in the proteome for each strain and/or treatment along with the number of differentially expressed transcripts between select conditions for *P. antarctica* strain 1871 and strain 1374. Proteins were identified using a 1% FDR (false discovery rate) threshold, a peptide threshold of 95%, and a minimum of two unique peptides per protein. The total number of peptide-to-spectrum matches (PSMs) is given for the total of each strain in parentheses. A threshold of three spectral counts in at least one of the treatments was selected for inclusion in the comparative analysis.

Strain	Treatment (Fe' pM)	Proteins identified (PSMs)
1871	2	204
	41	214
	120	234
	740	226
	1200	251
	3900	258
	Total	536 (28 887)
1374	2	581
	41	613
	120	600
	740	654
	1200	623
	3900	527
	Total	1085 (72 087)

calcium-binding proteins under low iron conditions suggests an important role for intracellular calcium, either in its involvement in flagellate motility and/or having a role in inhibiting cell abilities to form colonies while under iron limitation. This use of calcium signaling is notable given that calcium is a major constituent of seawater (0.01 mol L^{-1}), implying a need for efflux and exclusion of calcium from the cytoplasm.

3.5 *Phaeocystis antarctica* strain-specific responses

Phaeocystis antarctica is believed to have speciated from warm-water ancestors, and populations within the Antarctic are mixed via the rapid Antarctic Circumpolar Current (ACC, 1–2 years) circulation with the Ross Sea and Weddell Sea, which entrains strains nearly simultaneously (Lange et al., 2002). Moreover, high genetic diversity has been observed across a large number of *P. antarctica* isolates and even within isolates co-isolated from a bloom (Gäbler-Schwarz et al., 2015). Given the differences in geographic location of the isolates used in this study, there may be some differences regarding adaptation and ecological role between them. In the Ross Sea, *P. antarctica* dominates, and cells exhibit seasonal variability between flagellated states (early Spring, late summer) and colonial stage (late Spring–early summer) (Smith et al., 2003). In contrast, in the western Antarctic Penin-

sula, near the Weddell Sea from which strain 1871 was isolated (Palmer station), *P. antarctica* is outnumbered by diatoms and cryptomonads in terms of algal biomass, and colonies are generally rare (Ducklow et al., 2007). While global proteomic and transcriptomic analyses revealed differences among strains (Supplement Data 1), both strains had responses that overwhelmingly supported a concerted effort towards structural changes under high iron versus low iron, consistent with the minor phylogenetic differences previously reported for *P. antarctica* isolates due to rapid ACC circulation (Lange et al., 2002).

3.6 Examination of a *Phaeocystis* bloom metaproteome from the Ross Sea

The detailed laboratory studies above can be compared to a first metaproteomic analysis of a Ross Sea *Phaeocystis antarctica* bloom to provide an examination of the in situ ecology and biogeochemical and their underlying biochemical signatures. Due to the newness of metaproteomic eukaryotic phytoplankton research, some methodological detail has been incorporated into this section. For field analysis a net tow sample was collected north of Ross Island (Fig. 8) on 30 December 2005, in which *Phaeocystis* colonies were visually dominant. Temporal changes in the bloom composition have been described for this summer expedition and an austral spring expedition later that year (NBP06-01 and NBP06-08, respectively), and a shift was observed from a *P. antarctica*-dominated ecosystem to a mixture of *P. antarctica* and diatoms (Smith et al., 2013). Surface pigment distributions showed the sampling region to be within a particularly intense bloom dominated by *Phaeocystis* as observed by abundant 19'-hexanoyloxyfucoxanthin pigment (Fig. 8), reaching concentrations of 1096 ng L^{-1} and total chlorophyll *a* concentrations of 1860 ng L^{-1} on the sampling day. CHEMTAX analysis of these HPLC pigments found that *P. antarctica* populations accounted for approximately 88% of surface water total chlorophyll at this time. Fucoxanthin pigment, characteristic of diatoms, was lower here (136 ng L^{-1}) compared to samples from the western Ross Sea (Fig. 8), consistent with prior Ross Sea observations. Repeated sampling near the sampling region ($\sim 77.5^\circ \text{ S}$) 2 weeks after taking the metaproteome sample found lower overall chlorophyll *a* levels (Smith et al., 2013) consistent with bloom decay. Iron measured very near this location (76.82° S , 170.76° E also on 30 December 2005) revealed a surface dissolved iron concentration of 170 pM (6 m depth) and an acid-labile particulate iron concentration of 1590 pM (Sedwick et al., 2011), consistent with iron depletion in seawater following drawdown of the accumulated winter iron supply and incorporation of iron into biological particulate material (Noble et al., 2013; Sedwick et al., 2000).

The metaproteome analyses of the Ross Sea sample were conducted by bottom-up mass spectrometry analysis of tryptic peptides using initially a one-dimensional and subse-

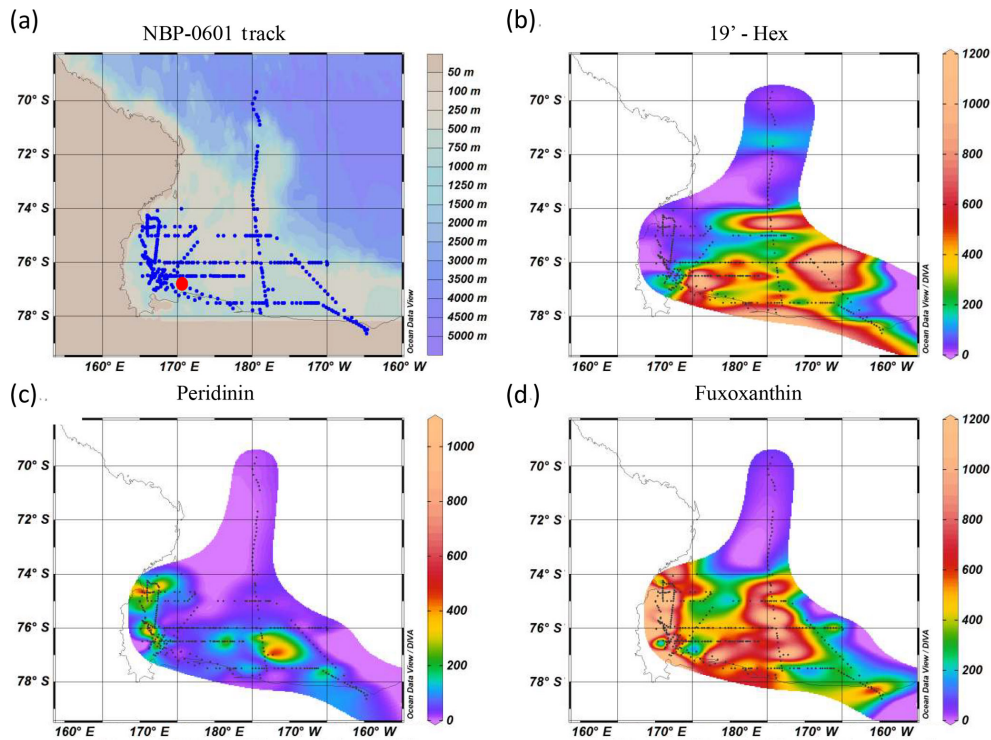


Figure 8. Location of the metaproteome sample and pigment data from a Ross Sea *Phaeocystis* bloom net tow sample. (a) Station map of NBP06-01 (27 December 2005 to 23 January 2006); the metaproteome sample was taken on 30 December by net tow location (red circle). (b) 19'-hexanoyloxyfucoxanthin (“19'-Hex”) pigment is associated with *Phaeocystis*, while (c) peridinin and (d) fucoxanthin pigments are typically associated with dinoflagellates and diatoms, respectively (although dinoflagellates living heterotrophically can be lacking in pigment). Comparisons of the spring and summer expeditions (NBP06-08 and NBP06-01, respectively) revealed a shift from being dominated by *P. antarctica* to being a mixture of *P. antarctica* and diatoms. See Smith et al. (2013) for further details.

quently a deeper two-dimensional chromatographic methodology (1-D and 2-D from here on), followed by peptide-to-spectrum matching of putative peptide masses and their fragment ions to predicted peptides from translated DNA sequences. While this approach is common for model organisms and has been successfully applied to primarily prokaryotic components of natural communities (Morris et al., 2010; Ram et al., 2005; Sowell et al., 2008; Williams et al., 2012), there continue to be challenges in metaproteomic analyses of diverse communities, particularly when including an extensive eukaryotic component such as is present in the Ross Sea phytoplankton bloom. VerBerkmoes et al. (2005) demonstrated the feasibility of using mass spectrometry metaproteomic analysis for the detection of eukaryotic proteins in a complex sample matrix. To address these issues, we utilized three sequence databases for peptide-to-spectrum matching (see Methods and Table S2). Analysis of both unique (tryptic) peptides and identified proteins are provided here, and unique peptides are particularly valuable in metaproteome interpretation as a basal unit of protein diversity that can be definitively compared across the three sequence databases (Saito et al., 2015).

The combined *P. antarctica* strain transcriptome database (Database 1) generated the largest number of protein and unique peptide identifications: 1545 and 3816 in 2-D (912 and 2103 in 1-D) (Table 2, Fig. 9a). This strong relative performance of the strain database was surprising and likely reflects the depth of the *P. antarctica* isolate transcriptomes and resultant translation into greater metaproteomic depth. Approximately 60 % of field identifications mapped to strain 1374 (57 %); a broad synthesis of all proteomes based on KOG annotations also indicated that the metaproteomes appeared most similar to the Ross Sea strain 1374 (Fig. S3). The Ross Sea metatranscriptome database (Database 2) resulted in 1475 proteins and 3210 unique peptides in 2-D analyses (859 proteins and 1520 unique peptides in 1-D) distributed across a large number of taxa, with 324 of those proteins associated with *P. antarctica*. The Antarctic bacterial metagenome database (Database 3) produced 102 proteins and 237 unique peptides in 2-D (98 proteins and 186 peptides in 1-D) that mapped to bacteria likely associated with the phytoplankton communities, given the use of a net that would not otherwise capture free-living bacteria. The low number of bacterial protein and peptide identifications could reflect their small abundance or limited metagenomic cover-

Table 2. Comparison of the total number of proteins, peptides, and spectra measured in the Ross Sea metaproteome net tow sample using three databases for peptide-to-spectrum matching (see Table S2). Results from two-dimensional and one-dimensional (1-D in parentheses) analyses are shown.

Peptide-to-spectrum match (PSM) database	Total proteins	Total unique peptides	Total spectra matched	Decoy FDR ^a percent (peptide level)
(1) <i>Phaeocystis</i> strains transcriptomes ^b	1545 (912)	3816 (2103)	14 088 (8226)	0.6 (0.17)
(2) Ross Sea metatranscriptome ^c	1474 (859)	3210 (1520)	10 154 (4725)	0.1 (0.7)
(3) Antarctic bacterial metagenomes ^d	102 (92)	237 (186)	530 (440)	3.6 (2.3)

^a FDR refers to the false discovery rate of a reversed peptide database. ^b Metaproteome annotated using the laboratory-generated transcriptomes for strain 1871 and strain 1374 (Database 1). ^c Metaproteome annotated using the metatranscriptome generated from sample split of original Ross Sea sample (Database 2). ^d Bacterial metaproteome annotated using bacterial metagenomes from Delmont et al. (2014) (Database 3).

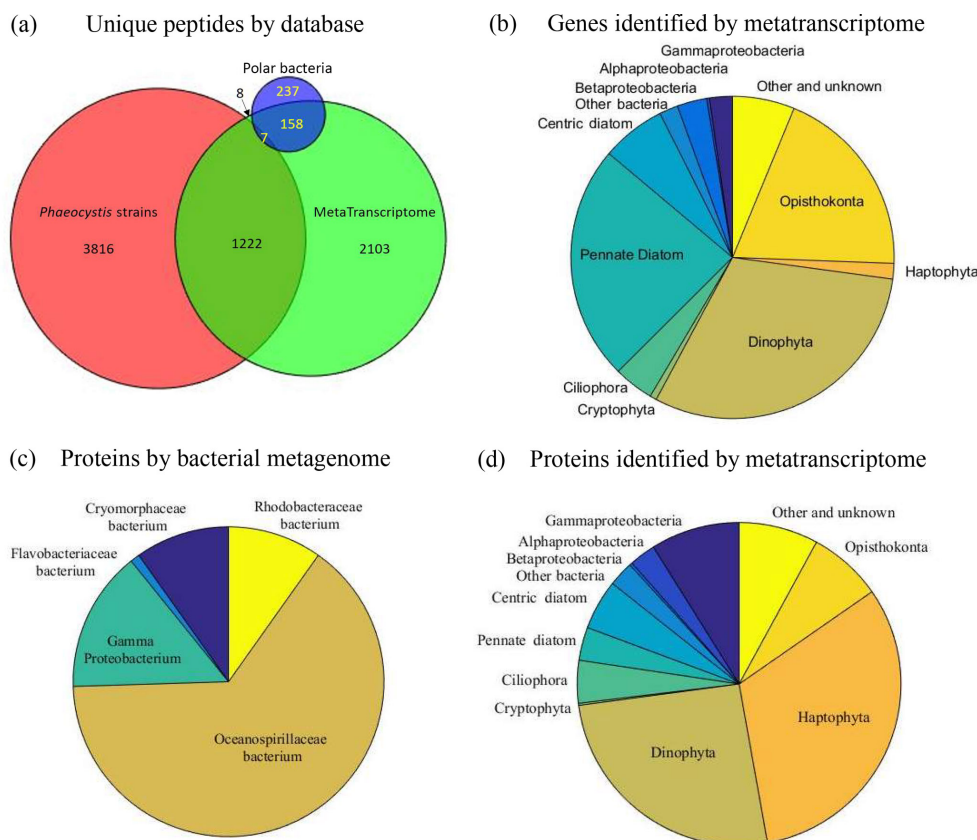


Figure 9. (a) Venn diagram of the attribution of the 5885 total unique peptides identified in the metaproteome sample to three DNA–RNA sequence databases (Table S2). (b) Taxon group composition of genes identified by metatranscriptome analyses (combining total RNA and polyA RNA fractions). (c) Taxon group composition of proteins identified by the bacterial metagenomic database (Database 3). (d) Taxon group composition of proteins identified by the metatranscriptome database (Database 2).

age. Due to the extensive diversity present, there was overlap between the peptide identifications from each database for the 5885 total unique peptides in 2-D (3193 in 1-D); 1222 (in 2-D; 544 in 1-D) *P. antarctica* peptides were shared between the *Phaeocystis* strain and Ross Sea metatranscriptome databases; 158 (in 2-D; 69 in 1-D) bacterial peptides were in common between the Ross Sea metatranscriptome and the bacterial metagenomic databases, followed by very

small numbers shared between bacterial metagenome and the *Phaeocystis* strains database searches (eight peptides in both 1-D and 2-D) and all three databases (seven and four peptides in 1-D and 2-D, respectively), likely due to a small fraction of tryptic peptides shared between diverse organisms (Saito et al., 2015).

This multi-database approach and the relatively low overlap illustrates the necessity of employing diverse sequence

databases that target distinct components of the biological community, as well as the value in coupling metatranscriptomic and metagenomic sequence databases to metaproteomic functional analysis to capture the extent of natural diversity. This is evident in the taxon group analysis, in which the metatranscriptome has a large representation of Dinophyta and diatoms and only a small contribution from Haptophyta that include *Phaeocystis*, likely due to the large genome sizes and transcription rates, particularly of dinoflagellates, and perhaps due to interferences of *Phaeocystis* RNA extraction due to the copious mucilage present (Fig. 9b). In contrast, the metaproteome derived from the metatranscriptome database is dominated by Haptophyta and Dinophyta, with minor contributions from other groups (Fig. 9d), reflecting the dominant organismal composition seen in the pigment analyses (Fig. 8). Due to a coarse net mesh size much larger than a typical bacterial cell, the bacterial community captured by these metatranscriptome and metaproteome analyses most likely reflects the microbiome associated with larger phytoplankton and protists, particularly within the abundant *P. antarctica* colonies. Databases 2 and 3 result in 211 and 102 bacterial protein identifications (in 2-D; 148 and 100 in 1-D), including representatives from Oceanospirillaceae, Rhodobacteraceae, Cryomorphaceae, *Flavobacteria*, and Gammaproteobacteria (Fig. 9c and d). The lower number of bacterial identifications could be due to low bacterial biomass in the net tow sample relative to phytoplankton biomass and/or limited metagenomics coverage.

This Ross Sea bloom metaproteome–metatranscriptome analysis provides a window into the complex interactions of this community with its chemical environment. *Phaeocystis antarctica* proteins were abundant in the sample with over 450 (in 2-D; 300 in 1-D) proteins identified, yet interestingly, we identified proteins associated with both high and low iron treatments, including those corresponding to flagellate and colonial life stages identified in the culture experiments (Figs. 10 and S1). This presence of both life cycle stages of *Phaeocystis* could be interpreted as evidence of an actively growing bloom, with growing flagellate cells coalescing to form new colonies, as well as a standing stock of colonial cells. As mentioned earlier, division and growth of *P. antarctica* colonies is believed to require transitioning back through the flagellate life cycle stage (Rosseau et al., 1994), and hence a mixed population of flagellate and colonial stages would be expected of a growing population, consistent with our laboratory observations (Fig. 3c).

The presence of well-known iron-sparing proteins such as plastocyanin (Fig. 10) was consistent with the depleted dissolved iron concentration (170 pM) in nearby surface waters that are closest to the 120 pM Fe³⁺ of the low iron treatments (Peers and Price, 2006; Sedwick et al., 2011), as well as incubation experiments on the same expedition initiated 3 days prior that demonstrated iron limitation of *P. antarctica* (and iron–B₁₂ colimitation of diatom) populations (Bertrand et al., 2007). Notably, the actual Fe³⁺ of the Ross Sea was likely

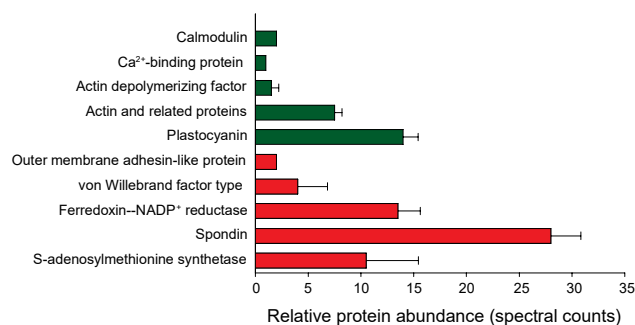


Figure 10. Putative biomarkers identified in the *Phaeocystis* metaproteome annotated using the field metatranscriptome (error bars represent SD of replicate samples; $n = 2$; 1-D dataset used). Green bars indicate putative “low iron” biomarkers; red bars indicate putative “high iron” biomarkers and correspond to the life cycle stages observed (Fig. 3).

considerably lower than this due to the presence of strong organic iron complexes (Boye et al., 2001). Strzeppek et al. found evidence for growth of *P. antarctica* and some polar diatoms on strong organic iron complexes at somewhat reduced growth rates in their culture experiments, implying a high-affinity iron acquisition system such as a ferric reductase, although the molecular components of such a system have yet to be identified in *P. antarctica* (Strzeppek et al., 2011). As described above, it is likely that both flagellate and colonial cell types have a need to manifest iron stress responses (e.g., distinct ISIPs found in the flagellate- and colonial-dominated cultures; Figs. 5 and 6) and that those distinct responses may be based on the extensive physical differences between life cycle phenotypes. The low contribution of chain-forming diatoms to this metaproteome sample was consistent with the higher sensitivity of some Ross Sea diatom strains to iron stress such as *Chaetoceros* (Fig. 3d) and the low iron availability. Careful examination of targeted mass spectrometry results (precursor and fragment ion analysis) for select iron proteins identified in culture studies showed consistently high-quality chromatograms within the field sample, demonstrating a capability to measure these potential peptide biomarkers within complex environmental samples in future field studies characterizing bloom and biogeochemical dynamics (Figs. 11 and S4–10).

The metaproteome analyses also captured relevant functional elements of the bacterial microbiome associated with the eukaryotic community based on the bacterial proteins identified in both the bacterial databases and the Ross Sea metatranscriptome (Fig. 9c and d). For example, the SAR92 clade of proteorhodopsin-containing heterotrophic bacteria was present (Stingl et al., 2007) and expressed both the iron storage protein bacterioferritin and TonB receptors, the latter of which are involved in siderophore and B₁₂ transport. In addition, the Fur iron regulon, iron-requiring ribonucleotide reductase, as well as the vitamin-related CobN cobalamin

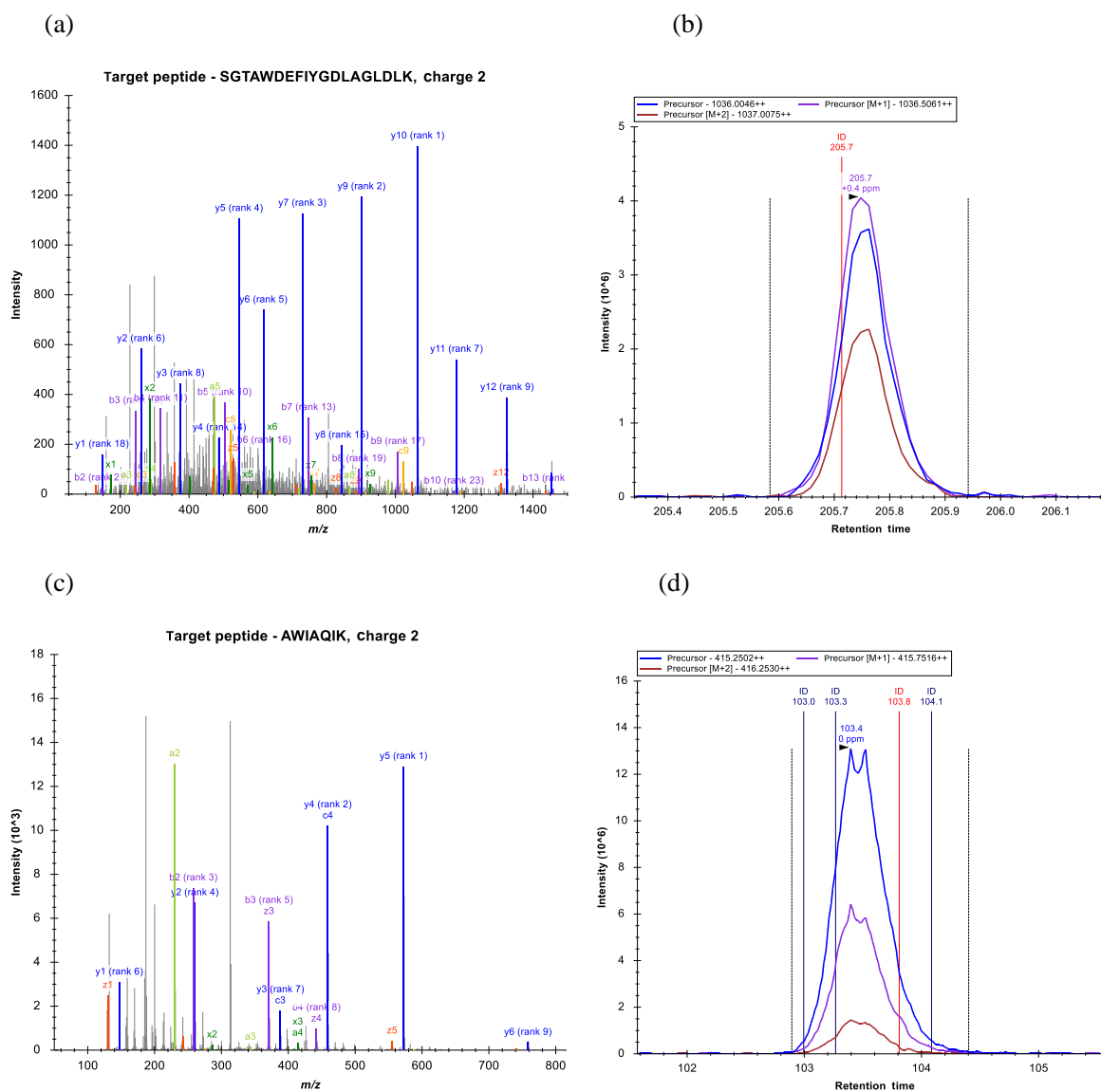


Figure 11. Example spectra and chromatograms of fragment ions for two peptides corresponding to a *P. antarctica* flavodoxin identified from the Ross Sea metaproteome sample (peptide sequences found within Database 1, 1871, contig_31444_1_606_+, 1374, contig_202625_47_661_+; Database 2, contig_175060_39_653_+). Peptide fragmentation spectra are shown in (a) and (c) and example chromatograms of MS1 intensities as well as with +1 and +2 mass addition for isotopic distributions are shown (b) and (d), demonstrating the utility of these iron stress biomarkers in field samples.

biosynthesis protein, B₁₂-requiring methyl-malonyl CoA, and thiamine ABC transporter were observed from several heterotrophic bacteria species including Oceanospirillaceae, Rhodobacteraceae, and Cryomorphaceae (Supplement Data 2) (Bertrand et al., 2015; Murray and Grzymiski, 2007). These results imply that heterotrophic bacteria known to be associated with the *Phaeocystis* colonies, such as SAR92 and Oceanospirillaceae, were also likely responding to micronutrients by concentrating and storing iron and through the biosynthesis of B₁₂. In doing so this bacterial

microbiome could have been harboring an “internal” source of micronutrients, fostering a mutualism with *Phaeocystis* colonies in exchange for a carbon source and consistent with the high particulate iron measured during this station (Sedwick et al., 2011). This could create a competitive advantage for *P. antarctica* relative to the iron and B₁₂-stressed diatoms for early season bloom formation, as previously hypothesized and observed in the Ross Sea in enrichment studies (Bertrand et al., 2007). Although diatoms were less prominent in the dataset, several diatom proteins identified

were indicative of the potential for iron stress (e.g., plastocyanin and ISIP3; Supplement Data 2); however, the diatom CBA1 cobalamin-acquisition protein was not identified in the metatranscriptome and hence would not be detected in the metaproteome using the current methods, but could be targeted in future studies from this dataset.

4 Conclusions

Phaeocystis antarctica is a major contributor to Southern Ocean primary productivity, yet arguably is one of the least well understood of key marine phytoplankton species. The multiple life cycle stages of *P. antarctica* add to its ecological and biochemical complexity. Here we have undertaken a detailed combined physiological and proteomic analysis enabled by transcriptomic sequencing under varying conditions of iron nutrition and compared these to an initial study of the metaproteome of a Ross Sea *Phaeocystis* bloom. These results demonstrate that *P. antarctica* has evolved to utilize elaborate capabilities to confront the widespread iron scarcity that occurs in the Ross Sea and Southern Ocean, including iron-metalloenzyme-sparing systems and the deployment of transport and other systems that appear to be unique to the flagellate and colonial morphotypes. To our surprise, increasing iron abundance triggered colony formation in one strain in this study, and visual and proteomic evidence implied the second strain was also attempting to do so. Prior studies have invoked light irradiance and mixed layer depth as key factors in colony production and the concurrent Ross Sea *P. antarctica* bloom initiation (Arrigo et al., 1999), and hence there may be other factors that could have this effect as well. These results also provide preliminary insight into the cellular restructuring processes that occur upon cellular metamorphosis between life cycle stages in *P. antarctica* and identify numerous dynamic proteins of unknown function for future study. Finally, this study demonstrates the potential for the application of coupled transcriptomic and proteomic biomarker methodologies in studying the ecology of microbial interactions (including iron and B₁₂) and their influence on biogeochemistry in complex polar ecosystems such as the Ross Sea. The improved molecular and biochemical understanding of *P. antarctica* and its response to iron provided here are valuable in the design of future experiments and targeted metaproteomic assays to examine natural populations and to improve understanding of environmental factors that influence the annual bloom formation of an important coastal ecosystem of the Southern Ocean.

Data availability. *Phaeocystis antarctica* RNA sequence data reported in this paper have been deposited in the NCBI sequence read archive (<https://www.ncbi.nlm.nih.gov/bioproject/PRJNA339150>, Bender et al., 2018a; <https://www.ncbi.nlm.nih.gov/bioproject/PRJNA339151>, Bender et al., 2018b) under BioProject accession no. PRJNA339150 and BioSample accession

nos. SAMN05580299–SAMN05580303. Ross Sea metatranscriptomes have been deposited under BioProject accession no. PRJNA339151 and BioSample accession nos. SAMN05580312–SAMN05580313. Proteomic data from the lab and field components were submitted to the Pride database (project name: *Phaeocystis antarctica* CCMP 1871 and CCMP 1374, Ross Sea *Phaeocystis* bloom, LC-MSMS; project accession: PXD00534 project <https://doi.org/10.6019/PXD005341>; Bender et al., 2018c).

The Supplement related to this article is available online at <https://doi.org/10.5194/bg-15-4923-2018-supplement>.

Author contributions. SJB contributed to data analysis and writing; DMM conducted the laboratory experiments and (meta)proteome extractions; MRM conducted the mass spectrometry sample preparation and processing; HZ conducted RNA extractions; JPM and JB contributed to transcriptome sequence analyses; GRD contributed to field measurements and paper edits; AEA contributed to the experimental design, data analysis, and writing; MAS contributed to field sample processing, experimental design, data analysis, and writing.

Competing interests. The authors declare that they have no conflict of interest.

Acknowledgements. Support for this study was provided by an Investigator grant to Mak A. Saito from the Gordon and Betty Moore Foundation (GBMF3782), National Science Foundation grants NSF-PLR 0732665, OCE-1435056, OCE-1220484, and ANT-1643684, the WHOI Coastal Ocean Institute, and a CINAR Postdoctoral Scholar Fellowship provided to Sara J. Bender through the Woods Hole Oceanographic Institution. Support was provided to Andrew E. Allen through NSF awards ANT-0732822, ANT-1043671, and OCE-1136477 and Gordon and Betty Moore Foundation grant GBMF3828. Additional support was provided to GRD through NSF award OPP-0338097. We are indebted to Roberta Marinelli for her leadership and vision. We would also like to thank Emily Lorch for her assistance with culturing, Julie Rose for generously sharing a net tow field sample, and Andreas Krupke for paper feedback.

Edited by: Christine Klaas

Reviewed by: two anonymous referees

References

- Abedin, M. and King, N.: Diverse and evolutionary paths to cell adhesion, *Trends Cell Biol.*, 20, 734–742, 2010.
- Alderkamp, A. C., Buma, A. G. J., and Van Rijssel, M.: The carbohydrates of *Phaeocystis* and their degradation in the microbial food web, *Biogeochemistry*, 83, 99–118, 2007.

- Alexander, H., Jenkins, B. D., Rynearson, T. A., Saito, M. A., Mercier, M. L., and Dyhrman, S. T.: Identifying reference genes with stable expression from high throughput sequence data, *Front Microbiol.*, 9, 385, <https://doi.org/10.3389/fmicb.2012.00385>, 2012.
- Allen, A. E., LaRoche, J., Maheswari, U., Lommer, M., Schauer, N., Lopez, P. J., Finazzi, G., Fernie, A. R., and Bowler, C.: Whole-cell response of the pennate diatom *Phaeodactylum tricornutum* to iron starvation, *P. Natl. Acad. Sci. USA*, 105, 10438–10443, 2008.
- Arrigo, K. R., Worthen, D., Schnell, A., and Lizotte, M. P.: Primary production in Southern Ocean waters, *J. Geophys. Res.*, 103, 15587–15600, 1998.
- Arrigo, K. R., Robinson, D. H., Worthen, D. L., Dunbar, R. B., R, D. G., vanWoert, M. L., and Lizotte, M. P.: Phytoplankton community structure and the drawdown of nutrients and CO₂ in the Southern Ocean, *Science*, 283, 365–367, <https://doi.org/10.1126/science.283.5400.365>, 1999.
- Arrigo, K. R., DiTullio, G. R., Dunbar, R. B., Robinson, D. H., vanWoert, M. L., Worthen, D. L., and Lizotte, M. P.: Phytoplankton taxonomic variability in nutrient utilization and primary production in the Ross Sea, *J. Geophys. Res.*, 105, 8827–8846, <https://doi.org/10.1029/1998JC000289>, 2000.
- Bender, S. J., Moran, D. M., McIlvin, M. R., Zheng, H., McCrow, J. P., Badger, J., DiTullio, G. R., Allen, A. E., and Saito, M. A.: *Phaeocystis antarctica* transcriptomes under iron limitation, available at: <https://www.ncbi.nlm.nih.gov/bioproject/PRJNA339150> (last access: 16 August 2016), 2018a.
- Bender, S. J., Moran, D. M., McIlvin, M. R., Zheng, H., McCrow, J. P., Badger, J., DiTullio, G. R., Allen, A. E., and Saito, M. A.: *Phaeocystis antarctica* Transcriptome or Gene expression, available at: <https://www.ncbi.nlm.nih.gov/bioproject/PRJNA339151> (last access: 16 August 2016), 2018b.
- Bender, S. J., Moran, D. M., McIlvin, M. R., Zheng, H., McCrow, J. P., Badger, J., DiTullio, G. R., Allen, A. E., and Saito, M. A.: *Phaeocystis antarctica* CCMP 1871 and CCMP 1374, Ross Sea *Phaeocystis* bloom, LC-MSMS, <https://doi.org/10.6019/PXD005341>, 2018c.
- Bertrand, E. M., Saito, M. A., Rose, J. M., Riesselman, C. R., Lohan, M. C., Noble, A. E., Lee, P. A., and R, D. G.: Vitamin B₁₂ and iron colimitation of phytoplankton growth in the Ross Sea, *Limnol. Oceanogr.*, 52, 1079–1093, 2007.
- Bertrand, E. M., Saito, M. A., Lee, P. A., Dunbar, R. B., Sedwick, P. N., and R, D. G.: Iron limitation of a springtime bacterial and phytoplankton community in the Ross Sea: Implications for Vitamin B₁₂ nutrition, *Front. Microbiol.*, 2, 1–12, <https://doi.org/10.3389/fmicb.2011.00160>, 2011.
- Bertrand, E. M., Moran, D. M., McIlvin, M. R., Hoffman, J. M., Allen, A. E., and Saito, M. A.: Methionine synthase interreplacement in diatom cultures and communities: Implications for the persistence of B₁₂ use by eukaryotic phytoplankton, *Limnol. Oceanogr.*, 58, 1431–1450, <https://doi.org/10.4319/lo.2013.58.4.1431>, 2013.
- Bertrand, E. M., McCrow, J. P., Moustafa, A., Zheng, H., McQuaid, J. B., Delmont, T. O., Post, A. F., Sipler, R. E., Spackeen, J. L., Xu, K., Bronk, D. A., Hutchins, D. A., and Allen, A. E.: Phytoplankton–bacterial interactions mediate micronutrient colimitation at the coastal Antarctic sea ice edge, *P. Natl. Acad. Sci. USA*, 112, 9938–9943, <https://doi.org/10.1073/pnas.1501615112>, 2015.
- Boye, M., van den Berg, C., de Jong, J., Leach, H., Croot, P., and de Baar, H. J. W.: Organic complexation of iron in the Southern Ocean, *Deep-Sea Res. Pt. I*, 48, 1477–1497, 2001.
- Chiovitti, A., Bacic, A., Burke, J., and Wetherbee, R.: Heterogeneous xylose-rich glycans are associated with extracellular glycoproteins from the biofouling diatom *Craspedostaurus australis* (Bacillariophyceae), *Eur. J. Phycol.*, 38, 351–360, <https://doi.org/10.1080/09670260310001612637>, 2003.
- Coale, K. H., Wang, X., Tanner, S. J., and Johnson, K. S.: Phytoplankton growth and biological response to iron and zinc addition in the Ross Sea and Antarctic Circumpolar Current along 170° W, *Deep-Sea Res. Pt. II*, 50, 635–653, 2003.
- Delmont, T. O., Hammar, K. M., Ducklow, H. W., Yager, P. L., and Post, A. F.: *Phaeocystis antarctica* blooms strongly influence bacterial community structures in the Amundsen Sea polynya, *Front. Microbiol.*, 5, 646, <https://doi.org/10.3389/fmicb.2014.00646>, 2014.
- DiTullio, G. R., Grebmeier, J. M., Arrigo, K. R., Lizotte, M. P., Robinson, D. H., Leventer, A., Barry, J. P., vanWoert, M. L., and Dunbar, R. B.: Rapid and early export of *Phaeocystis antarctica* blooms in the Ross Sea, Antarctica, *Nature*, 404, 595–598, <https://doi.org/10.1038/35007061>, 2000.
- Drake, J. L., Mass, T., Haramaty, L., Zelzion, E., Bhattacharya, D., and Falkowski, P. G.: Proteomic analysis of skeletal organic matrix from the stony coral *Stylophora pistillata*, *P. Natl. Acad. Sci. USA*, 110, 3788–3793, 2013.
- Ducklow, H. W., Baker, K., Martinson, D. G., Quetin, L. B., Ross, R. M., Smith, R. C., Stammerjohn, S. E., Vernet, M., and Fraser, W.: Marine pelagic ecosystems: the West Antarctic Peninsula, *Philos. T. Roy. Soc. B*, 362, 67–94, <https://doi.org/10.1098/rstb.2006.1955>, 2007.
- Dunbar, R. B., Leventer, A. R., and Mucciarone, D. A.: Water column sediment fluxes in the Ross Sea, Antarctica: Atmospheric and sea ice forcing, *J. Geophys. Res.*, 103, 30741–30759, <https://doi.org/10.1029/1998JC900001>, 1998.
- Eng, J. K., McCormack, A. L., and Yates, J. R.: An approach to correlate tandem mass spectral data of peptides with amino acid sequences in a protein database, *J. Am. Soc. Mass Spectrom.*, 5, 976–989, [https://doi.org/10.1016/1044-0305\(94\)80016-2](https://doi.org/10.1016/1044-0305(94)80016-2), 1994.
- Ewenstein, B. M.: Von Willebrand's disease, *Annu. Rev. Med.*, 48, 525–542, <https://doi.org/10.1146/annurev.med.48.1.525>, 1997.
- Feng, Y., Hare, C. E., Rose, J. M., Handy, S. M., DiTullio, G. R., Lee, P. A., Smith Jr., W. O., Peloquin, J., Tozzi, S., Sun, J., Zhang, Y., Dunbar, R. B., Long, M. C., Sohst, B., Lohan, M., and Hutchins, D. A.: Interactive effects of iron, irradiance and CO₂ on Ross Sea phytoplankton, *Deep-Sea Res. Pt. I*, 57, 368–383, <https://doi.org/10.1016/j.dsr.2009.10.013>, 2010.
- Gäbler-Schwarz, S., Medlin L. K., and Leese, F.: A puzzle with many pieces: the genetic structure and diversity of *Phaeocystis antarctica* Karsten (Prymnesiophyta), *Eur. J. Phycol.*, 50, 112–124, <https://doi.org/10.1080/09670262.2014.998295>, 2015.
- Garcia, N. S., Sedwick, P. N., and DiTullio, G. R.: Influence of irradiance and iron on the growth of colonial *Phaeocystis antarctica*: implications for seasonal bloom dynamics in the Ross Sea, Antarctica, *Aquat. Microb. Ecol.*, 57, 203–220, 2009.
- Garrison, D. L., Gibson, A., Kunze, H., Gowing, M. M., Vickers, C. L., Mathot, S., and Bayre, R. C.: The Ross Sea Polynya Project:

- Diatom- and Phaeocystis-dominated phytoplankton assemblages in the Ross Sea, Antarctica, 1994–1996, *Biogeochemistry of the Ross Sea*, 53–76, 2003.
- Hallmann, A.: Extracellular matrix and sex-inducing pheromone in *Volvox*, *Int. Rev. Cytol.*, 227, 131–182, 2003.
- Hamm, C. E.: Architecture, ecology and biogeochemistry of *Phaeocystis* colonies, *J. Sea Res.*, 43, 307–315, 2000.
- Hamm, C. E., Simson, D. A., Merkel, R., and Smetacek, V.: Colonies of *Phaeocystis globosa* are protected by a thin but tough skin, *Mar. Ecol.-Prog. Ser.*, 187, 101–111, 1999.
- Hayward, D. C., Hetherington, S., Behm, C. A., Grasso, L. C., Forêt, S., Miller, D. J., and Ball, E. E.: Differential gene expression at coral settlement and metamorphosis - A subtractive hybridization study, *PLoS ONE*, 6, e26411, <https://doi.org/10.1371/journal.pone.0026411>, 2011.
- Jacobsen, A., Larsen, A., Martínez-Martínez, J., Verity, P. G., and Frischer, M. E.: Susceptibility of colonies and colonial cells of *Phaeocystis pouchetii* (Haptophyta) to viral infection, *Aquat. Microb. Ecol.*, 48, 105–112, 2007.
- King, N., Hittinger, C. T., and Carroll, S. B.: Evolution of key cell signaling and adhesion protein families predates animal origins, *Science*, 301, 361–363, <https://doi.org/10.1126/science.1083853>, 2003.
- Kröger, N., Bergsdorf, C., and Sumper, M.: A new calcium binding glycoprotein family constitutes a major diatom cell wall component, *EMBO J.*, 13, 4676–4683, 1994.
- Lagerheim, G.: Ueber *Phaeocystis poucheti* (Har.) Lagerh., eine Plankton-Flagellate, *Oeivers af Vet Akad Foerhandl*, 4, 277–288, 1896.
- Lange, M., Chen, Y.-Q., and Medlin, L. K.: Molecular genetic delineation of *Phaeocystis* species (Prymnesiophyceae) using coding and non-coding regions of nuclear and plastid genomes, *Eur. J. Phycol.*, 37, 77–92, <https://doi.org/10.1017/S0967026201003481>, 2002.
- Lê, S., Josse, J., and Husson, F.: FactoMineR: an R package for multivariate analysis, *J. Stat. Softw.*, 25, 1–18, <https://doi.org/10.18637/JSS.v025:01>, 2008.
- Long, J. D., Smalley, G. W., Barsby, T., Anderson, J. T., and Hay, M. E.: Chemical cues induce consumer-specific defenses in a bloom-forming marine phytoplankton, *P. Natl. Acad. Sci. USA*, 104, 10512–10517, 2007.
- Lovenduski, N. S., Gruber, N., and Doney, S. C.: Toward a mechanistic understanding of the decadal trends in the Southern Ocean carbon sink, *Global Biogeochem. Cy.*, 22, GB3016, <https://doi.org/10.1029/2007GB003139>, 2008.
- Lubbers, G., Gieskes, W., Del Castilho, P., Salomons, W., and Bril, J.: Manganese accumulation in the high pH microenvironment of *Phaeocystis* sp. (Haptophyceae) colonies from the North Sea, *Mar. Ecol.-Prog. Ser.*, 59, 285–293, 1990.
- Luxem, K. E., Ellwood, M. J., and Strzepak, R. F.: Intraspecific variability in *Phaeocystis antarctica*'s response to iron and light stress, *PLoS ONE*, 12, e0179751, <https://doi.org/10.1017/journal.pone.0179751>, 2017.
- Martin, J. H., Fitzwater, S. E., and Gordon, R. M.: Iron deficiency limits phytoplankton growth in Antarctic waters, *Global Biogeochem. Cy.*, 4, 5–12, <https://doi.org/10.1029/GB004i001p00005>, 1990.
- Matrai, P. A., Vernet, M., Hood, R., Jennings, A., Brody, E., and Saemundsdottir, S.: Light-dependence of carbon and sulfur production by polar clones of the genus *Phaeocystis*, *Mar. Biol.*, 124, 157–167, 1995.
- Maucher, J. M. and DiTullio, G. R.: Flavodoxin as a Diagnostic Indicator of Chronic Fe-Limitation in the Ross Sea and New Zealand Sector of the Southern Ocean, *Biogeochemistry in the Ross Sea*, edited by: DiTullio, G. R. and Dunbar, R. B., Washington DC, AGU, 209–220, 2003.
- Michel, G., Tonon, T., Scornet, D., Cock, J. M., and Kloareg, B.: The cell wall polysaccharide metabolism of the brown alga *Ectocarpus siliculosus*. Insights into the evolution of extracellular matrix polysaccharides in Eukaryotes, *New Phytol.*, 188, 82–97, 2010.
- Morris, R. M., Nunn, B. L., Frazar, C., Goodlett, D. R., Ting, Y. S., and Rocap, G.: Comparative metaproteomics reveals ocean-scale shifts in microbial nutrient utilization and energy transduction, *ISME J.*, 4, 673–685, <https://doi.org/10.1038/ismej.2010.4>, 2010.
- Morrissey, J., Sutak, R., Paz-Yepes, J., Tanaka, A., Moustafa, A., Veluchamy, A., Thomas, Y., Botbol, H., Bouget, F.-Y., McQuaid, J. B., Tirichine, L., Allen, A. E., Lesuisse, E., and Bowler, C.: A novel protein, ubiquitous in marine phytoplankton, concentrates iron at the cell surface and facilitates uptake, *Curr. Biol.*, 25, 364–371, <https://doi.org/10.1016/j.cub.2014.12.004>, 2015.
- Murray, A. E. and Grzymiski, J. J.: Diversity and genomics of Antarctic marine micro-organisms, *Philos. T. Roy. Soc. B*, 362, 2259–2271, <https://doi.org/10.1098/rstb.2006.1944>, 2007.
- Noble, A. E., Moran, D. M., Allen, A. E., and Saito, M. A.: Dissolved and particulate trace metal micronutrients under the McMurdo Sound seasonal sea ice: basal sea ice communities as a capacitor for iron, *Front. Chem.*, 1, 1–18, <https://doi.org/10.3389/fchem.2013.00025>, 2013.
- Peers, G. and Price, N. M.: Copper-containing plastocyanin used for electron transport by an oceanic diatom, *Nature*, 441, 341–344, <https://doi.org/10.1038/nature04630>, 2006.
- Podell, S. and Gaasterland, T.: DarkHorse: a method for genome-wide prediction of horizontal gene transfer, *Genome Biol.*, 8, R16, <https://doi.org/10.1186/gb-2007-8-2-r16>, 2007.
- Ram, R. J., VerBerkmoes, N. C., Thelen, M. P., Tyson, G. W., Baker, B. J., Blake, R. C., Shah, M., Hettich, R., and Banfield, J.: Community proteomics of a natural microbial biofilm, *Science*, 308, 1915–1920, <https://doi.org/10.1126/science.2005>.
- Rho, M., Tang, H., and Ye, Y.: FragGeneScan: predicting genes in short and error-prone reads, *Nucleic Acids Res.*, 38, e191–e191, <https://doi.org/10.1093/nar/gkq747>, 2010.
- Riegman, R. and van Boekel, W.: The ecophysiology of *Phaeocystis globosa*: a review, *J. Sea Res.*, 35, 235–242, 1996.
- Riegman, R., Noordeloos, A. A. M., and Cadee, G. C.: *Phaeocystis* blooms and eutrophication of the continental coastal zones of the North Sea, *Mar. Biol.*, 112, 479–484, <https://doi.org/10.1007/BF00356293>, 1992.
- Roche, J. L., Boyd, P. W., McKay, R. M. L., and Geider, R. J.: Flavodoxin as an *in situ* marker for iron stress in phytoplankton, *Nature*, 382, 802–805, <https://doi.org/10.1038/382802a0>, 1996.
- Rousseau, V., Mathot, S., and Lancelot, C.: Calculating carbon biomass of *Phaeocystis* sp. from microscopic observations, *Mar. Biol.*, 107, 305–314, 1990.
- Rousseau, V., Vaulot, D., Casotti, R., Cariou, V., Lenz, J., Gunkel, J., and Baumann, M. The Life Cycle of *Phaeocystis* (Prymnesio-

- phyceae): Evidence and Hypotheses, *J. Marine Syst.*, 5, 23–39, 10.1016/0924-7963(94)90014-0, 1994.
- Rousseau, V., Chrétiennot-Dinet, M.-J., Jacobsen, A., Verity, P. G., and Whipple, S.: The life cycle of *Phaeocystis*: state of knowledge and presumptive role in ecology, *Biogeochemistry*, 83, 29–47, <https://doi.org/10.1007/s10533-007-9085-3>, 2007.
- Saito, M. A., Goepfert, T. J., Noble, A. E., Bertrand, E. M., Sedwick, P. N., and DiTullio, G. R.: A seasonal study of dissolved cobalt in the Ross Sea, Antarctica: micronutrient behavior, absence of scavenging, and relationships with Zn, Cd, and P, *Biogeosciences*, 7, 4059–4082, <https://doi.org/10.5194/bg-7-4059-2010>, 2010.
- Saito, M. A., McIlvin, M. R., Moran, D. M., Goepfert, T. J., R, D. G., Post, A. F., and Lamborg, C. H.: Multiple nutrient stresses at intersecting Pacific Ocean biomes detected by protein biomarkers, *Science*, 345, 1173–1177, 2014.
- Saito, M. A., Dorsk, A., Post, A. F., McIlvin, M. R., Rappé, M. S., R, D. G., and Moran, D. M.: Needles in the blue sea: Subspecies specificity in targeted protein biomarker analyses within the vast oceanic microbial metaproteome, *Proteomics*, 15, 3521–3531, <https://doi.org/10.1002/pmic.201400630>, 2015.
- Sarmiento, J. L., Hughes, T. M. C., Stouffer, R. J., and Manabe, S.: Simulated response of the ocean carbon cycle to anthropogenic climate warming, *Nature*, 393, 245–249, <https://doi.org/10.1038/30455>, 1998.
- Schoemann, V., Wollast, R., Chou, L., and Lancelot, C.: Effects of photosynthesis on the accumulation of Mn and Fe by *Phaeocystis* colonies, *Limnol. Oceanogr.*, 46, 1065–1076, 2001.
- Schoemann, V., Becquevort, S., Stefels, J., Rousseau, V., and Lancelot, C.: *Phaeocystis* blooms in the global ocean and their controlling mechanisms: a review, *J. Sea Res.*, 53, 43–66, 2005.
- Sedwick, P. N. and DiTullio, G. R.: Regulation of algal blooms in Antarctic shelf waters by the release of iron from melting sea ice, *Geophys. Res. Lett.*, 24, 2515–2518, <https://doi.org/10.1029/97GL02596>, 1997.
- Sedwick, P. N., DiTullio, G. R., and Mackey, D. J.: Iron and manganese in the Ross Sea, Antarctica: Seasonal iron limitation in Antarctic shelf waters, *J. Geophys. Res.*, 105, 11321–11336, <https://doi.org/10.1029/2000JC000256>, 2000.
- Sedwick, P. N., Garcia, N. S., Riseman, S. F., Marsay, C. M., and DiTullio, G. R.: Evidence for high iron requirements of colonial *Phaeocystis antarctica* at low irradiance, *Biogeochemistry*, 83, 83–97, <https://doi.org/10.1007/s10533-007-9081-7>, 2007.
- Sedwick, P. N., Marsay, C. M., Sohst, B. M., Aguilar Islas, A. M., Lohan, M. C., Long, M. C., Arrigo, K. R., Dunbar, R. B., Saito, M. A., Smith, W. O., and DiTullio, G. R.: Early season depletion of dissolved iron in the Ross Sea polynya: Implications for iron dynamics on the Antarctic continental shelf, *J. Geophys. Res.*, 116, C12019, <https://doi.org/10.1029/2010JC006553>, 2011.
- Smith Jr., W. O., Codispoti, L. A., Nelson, D. M., Manley, T., Buskey, E. J., Niebauer, H. J., and Cota, G. F.: Importance of *Phaeocystis* blooms in the high-latitude ocean carbon cycle, *Nature*, 352, 514–516, 1991.
- Smith Jr., W. O., Dennett, M. R., Mathot, S., and Caron, D. A.: The temporal dynamics of the flagellated and colonial stages of *Phaeocystis antarctica* in the Ross Sea, *Deep-Sea Res. Pt. II*, 50, 605–617, 2003.
- Smith, W. O., Tozzi, S., Long, M. C., Sedwick, P. N., Peloquin, J. A., Dunbar, R. B., Hutchins, D. A., Kolber, Z., and R, D. G.: Spatial and temporal variations in variable fluorescence in the Ross Sea (Antarctica): Oceanographic correlates and bloom dynamics, *Deep-Sea Res. Pt. I*, 79, 141–155, 2013.
- Solomon, C. M., Lessard, E. J., Keil, R. G., and Foy, M. S.: Characterization of extracellular polymers of *Phaeocystis globosa* and *P. antarctica*, *Mar. Ecol.-Prog. Ser.*, 250, 81–89, 2003.
- Sowell, S. M., Wilhelm, L. J., Norbeck, A. D., Lipton, M. S., Nicora, C. D., Barofsky, D. F., H, C., Smith, R. D., and Giovanonni, S. J.: Transport functions dominate the SAR11 metaproteome at low-nutrient extremes in the Sargasso Sea, *ISME J.*, 3, 93–105, <https://doi.org/10.1038/ismej.2008.83>, 2008.
- Stingl, U., Desiderio, R. A., Cho, J. C., Vergin, K. L., and Giovannoni, S. J.: The SAR92 Clade: an Abundant Coastal Clade of Culturable Marine Bacteria Possessing Proteorhodopsin, *Appl. Environ. Microbiol.*, 73, 2290–2296, <https://doi.org/10.1128/AEM.02559-06>, 2007.
- Strzepek, R. F., Maldonado, M. T., Hunter, K. A., Frew, R. D., and Boyd, P. W.: Adaptive strategies by Southern Ocean phytoplankton to lessen iron limitation: Uptake of organically complexed iron and reduced cellular iron requirements, *Limnol. Oceanogr.*, 56, 1983–2002, <https://doi.org/10.4319/lo.2011.56.6.1983>, 2011.
- Sunda, W. and Huntsman, S.: Effect of pH, light, and temperature on Fe–EDTA chelation and Fe hydrolysis in seawater, *Mar. Chem.*, 84, 35–47, [https://doi.org/10.1016/S0304-4203\(03\)00101-4](https://doi.org/10.1016/S0304-4203(03)00101-4), 2003.
- Sunda, W. G. and Huntsman, S. A.: Iron uptake and growth limitation in oceanic and coastal phytoplankton, *Mar. Chem.*, 50, 189–206, 1995.
- Thingstad, F. and Billen, G.: Microbial degradation of *Phaeocystis* material in the water column, *J. Marine Syst.*, 5, 55–65, [https://doi.org/10.1016/0924-7963\(94\)90016-7](https://doi.org/10.1016/0924-7963(94)90016-7), 1994.
- Tzarfati-Majar, V., Burstyn-Cohen, T., and Klar, A.: F-spondin is a contact-repellent molecule for embryonic motor neurons, *P. Natl. Acad. Sci. USA*, 98, 4722–4727, 2011.
- van Boekel, W.: *Phaeocystis* colony mucus components and the importance of calcium ions for colony stability, *Mar. Ecol.-Prog. Ser.*, 87, 301–305, 1992.
- Vardi, A.: Cell signaling in marine diatoms, *Communicative & Integrative Biology*, 1, 134–136, <https://doi.org/10.1016/j.cub.2008.05.037>, 2008.
- VerBerkmoes, N. C., Hervey, W. J., Shah, M., Land, M., Hauser, L., Larimer, F. W., Van Berkel, G. J., and Goeringer, D. E.: Evaluation of “shotgun” proteomics for identification of biological threat agents in complex environmental matrixes: experimental simulations, *Anal. Chem.*, 77, 923–932, 2005.
- Verity, P. G., Brussaard, C. P., Nejstgaard, J. C., van Leeuwe, M. A., Lancelot, C., and Medlin, L. K.: Current understanding of *Phaeocystis* ecology and biogeochemistry, and perspectives for future research, *Biogeochemistry*, 83, 311–330, <https://doi.org/10.1007/s10533-007-9090-6>, 2007.
- Warnes, G. R., Bolker, B., Bonebakker, L., Gentleman, R., Huber, W., Liaw, A., Lumley, T., Maechler, M., Magnusson, A., Moeller, S., and Schwartz, M.: gplots: Various R programming tools for plotting data, R package version, 2, 2009.
- Watanabe, Y., Hayashi, M., Yagi, T., and Kamiya, R.: Turnover of actin in *Chlamydomonas* flagella detected by fluores-

- cence recovery after photobleaching (frap), *Cell*, 29, 67–72, <https://doi.org/10.1247/csf.29.67>, 2004.
- Whitney, L. P., Lins, J. J., Hughes, M. P., Wells, M. L., Chappell, P. D., and Jenkins, B. D.: Characterization of putative iron responsive genes as species-specific indicators of iron stress in *Thalassiosiroid* diatoms, *Front. Microbiol.*, 2, 1–14, <https://doi.org/10.3389/fmicb.2011.00234>, 2011.
- Williams, T. J., Long, E., Evans, F., DeMaere, M. Z., Lauro, F. M., Raftery, M. J., Ducklow, H., Grzymiski, J. J., Murray, A. E., and Cavicchioli, R.: A metaproteomic assessment of winter and summer bacterioplankton from Antarctic Peninsula coastal surface waters, *ISME J.*, 6, 1883–1900, <https://doi.org/10.1038/ismej.2012.28>, 2012.
- Wu, Z., Jenkins, B. D., Rynearson, T. A., Dyhrman, S. T., Saito, M. A., Mercier, M., and Whitney, L. P.: Empirical bayes analysis of sequencing-based transcriptional profiling without replicates, *BMC Bioinformatics*, 11, 564, <https://doi.org/10.1186/1471-2105-11-564>, 2010.
- Zilliges, Y., Kehr, J. C., Mikkat, S., Bouchier, C., de Marsac, N. T., Borner, T., and Dittmann, E.: An extracellular glycoprotein is implicated in cell-cell contacts in the toxic cyanobacterium *Microcystis aeruginosa* PCC 7806, *J. Bacteriol.*, 190, 2871–2879, <https://doi.org/10.1128/JB.01867-07>, 2008.
- Zingone, A., Chrétiennot-Dinet, M.-J., Lange, M., and Medlin, L.: Morphological and genetic characterization of *Phaeocystis cordata* and *P. jahnii* (prymnesiophyceae), two new species from the Mediterranean Sea, *J. Phycol.*, 35, 1322–1337, <https://doi.org/10.1046/j.1529-8817.1999.3561322.x>, 1999.
- Zurbriggen, M. D., Tognetti, V. B., Fillat, M. F., Hajirezaei, M.-R., Valle, E. M., and Carrillo, N.: Combating stress with flavodoxin: a promising route for crop improvement, *Trends Biotechnol.*, 26, 531–537, 2008.